Modeling and Analysis of Non-Pneumatic Tires for Military Wheeled Vehicles

Author

MUBASHIR JALEEL

Regn No 00000238712

Supervisor

DR. RAJA AMER AZIM

DEPARTMENT OF MECHANICAL ENGINEERING
COLLEGE OF ELECTRICAL & MECHANICAL ENGINEERING
NATIONAL UNIVERSITY OF SCIENCES AND TECHNOLOGY
ISLAMABAD

MARCH, 2020

Modeling and Analysis of Non-Pneumatic Tires for Military Wheeled Vehicles

Author

MUBASHIR JALEEL

Regn No 00000238712

A dissertation submitted in partial fulfillment of the requirements for the degree of MS Mechanical Engineering

Thesis Supervisor:
DR. RAJA AMER AZIM

Thesis Supervisor's Signature: _____

DEPARTMENT OF MECHANICAL ENGINEERING
COLLEGE OF ELECTRICAL & MECHANICAL ENGINEERING
NATIONAL UNIVERSITY OF SCIENCES AND TECHNOLOGY,
ISLAMABAD

MARCH, 2020

Declaration

I certify that this research work titled "*Modeling and Analysis of Non-Pneumatic Tires for Military Wheeled Vehicles"* is my own work. The work has not been presented elsewhere for assessment. The material that has been used from other sources it has been properly acknowledged / referred.

Signature of Student
Mubashir Jaleel
Regn No 00000238712

Copyright Statement

Acknowledgements

I am thankful to my Almighty Allah to have guided me throughout this work at every step and for every new thought which You setup in my mind to improve it. Indeed, I could have done nothing without Your priceless help and guidance. Whosoever helped me throughout the course of my thesis, whether my parents or any other individual was Your will, so indeed none be worthy of praise but You.

I am profusely thankful to my beloved parents who raised me when I was not capable of walking and continued to support me throughout in every department of my life. I also extend my gratitude to my wife, who fully supported me during work on this thesis.

I would also like to express special thanks to my supervisor Dr. Raja Amer Azim for his help throughout my thesis. Without his help I wouldn't have been able to complete my thesis. I appreciate his patience and guidance during the whole thesis.

I would also like to thank Dr. Hasan Aftab Saeed and Dr. Syed Gul Hassan Naqvi for being on my thesis guidance and evaluation committee.

Finally, I would like to express my gratitude to all the individuals who have rendered valuable assistance to my study.

Dedicated to my parents and wife,

with whose prayers and support this work became possible

Abstract

Tire plays and important role in handling and stability of vehicles. Pneumatic tires are in use since more than a century, however they have certain limitations due to use of air. Loss of air, caused by puncture or in worse case a tire burst, can instigate severe instabilities for vehicles resulting in loss of precious lives and damage to expensive equipment. It may also severely affect availability of vehicles during military operational and civil rescue missions. Non-pneumatic tires (NPTs) have excellent potential of replacing pneumatic tires due to exclusion of these limitations. In this thesis, steady state cornering characteristics of a NPT with hexagonal lattice spokes is studied using finite element modeling and simulation. Cornering of the NPT is performed at various slip angles under different loads. Cornering characteristics of the NPT calculated through finite element analysis (FEA) are compared with those of a pneumatic tire of similar size. Results of the FEA show that analyzed NPT has higher cornering stiffness than the pneumatic tire.

NPT characteristics obtained through FEA are used in a commercial vehicle dynamics software to study it effects on handling and stability of vehicle. Dynamic behavior of vehicles with non-pneumatic and pneumatic tire is simulated and compared through standard vehicle testing procedures. Results of vehicle test procedures indicate a significant improvement in handling of vehicle due to use of NPTs. This study can assist in handling and availability oriented selection of tires for military wheeled vehicles.

Key Words: *Non-pneumatic tire, Hexagonal lattice spoke, Cornering characteristics, Finite element modeling*

Table of Contents

List of Figures

List of Tables

CHAPTER 1: INTRODUCTION AND MOTIVATION

1.1 Background

Tires are among the most important components of a ground vehicle. These are solely responsible for vehicle interaction with the ground. Tires perform certain important functions for the vehicle. They provide rolling support to the vehicle while maintaining desired ground clearance, transmit appropriate traction and braking to the vehicle for smooth operation. Tires provide a cushioning effect against road irregularities and forces generated during interaction with the ground. Tires are in use since early ages in one form or the other, from primitive use of logs to rigid wheel and further improvement in the form of pneumatic tires, they have been the base of transportation means.

Pneumatic tire(PT) was invented due to low power consumption, less noise, high vertical compliance, and speed, however it has certain limitations due to use of air. One of the major limitations of a pneumatic tire is pneumatic tire burst which may be catastrophic at high speeds. According to data, tire failures cause 46% of accidents at highways, out of these highway accidents 70% accidents are contributed by the bursting of tires. Mortality rate was near 100% for the accidents which were caused by tire burst for speeds more than 160 Km/h (Zhao, Zang, Chen, Li, & Wang, 2015). Non-availability of a vehicle due to flat or burst tire can heavily jeopardize the civil rescue or military operational missions. Replacement of pneumatic tire have been wanted by the researchers since early 1900s. Number of designs were presented but none could meet the required durability and ride quality of a pneumatic tire(Pajtas, 1990). Since the presentation of Tweel (combination of tire and wheel(Michelin, 2012), non-pneumatic tire (NPTs) have received increasing response due to their potential advantages described by the researchers, including no requirement for maintenance of air pressure, no punctures, no tire burst and lesser rolling resistance in comparison with PTs(Jin et al., 2018).

Design of NPT can be of two basic types. First design can be locally deflecting, which covers the road abnormalities by dislocation of comparatively smaller region of NPT, while second one is the design which can be globally deflecting that covers the road irregularities by spreading the dislocation through circumference of tire. The NPT design defined in present research falls into the category which deflect locally (Pajtas, 1990).

1.2 Design of a Non-Pneumatic Tire (NPT)

NPT don't have any strict description in literature. However, in contrast to the rigid wheel, it consists of a compliant structure which don't rely on the gas to support the weight of vehicle. NPT rely on flexible spokes to have compliance in vertical direction.

1.2.1 Structure

A typical NPT shown in Figure 1.1 consists of following parts(Rhyne & Cron, 2006): -

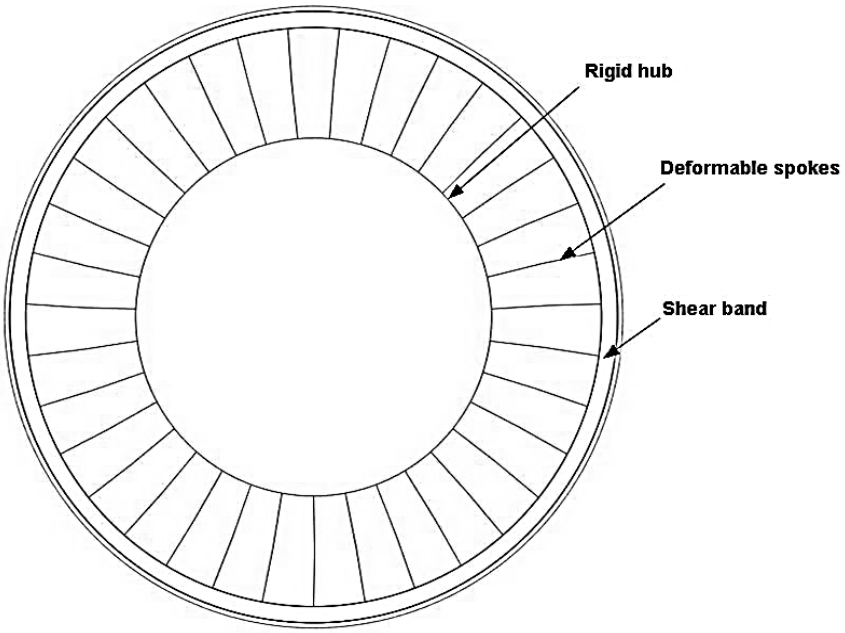

Figure 1.1: Structure of a NPT

(Rhyne & Cron, 2006)

a. **Hub**

Metals like an alloy or hard steel is generally used to make hub. Hub may be considered as rigid in comparison with other NPT components.

b. **Flexible spokes**

Support required by the NPT from top is provided by flexible spokes in tension. These spokes buckle under loading therefore these don't take load in compression. Spokes are generally uniform, flexible and fatigue resistant to undergo repeated cycles of compression, bending, buckling and extension. Due to these repeated cycles they pose a challenge to designers and manufacturers. Spokes of NPTs are generally made of polyurethane(PU)(Jin et al., 2018).

c. **Composite ring**

A NPT has an inner and an outer reinforcement, generally made of high strength steel. Composite ring is formed by sandwiching a shear layer in between these two reinforcements. Flexible properties of this ring works as a replacement of the air pressure in PTs. Shear ring enables a uniform contact pressure and avoids contact of spokes with road. Since PU has lesser viscoelastic energy loss therefore it is generally used as shear layer to reduce rolling resistance of tire(Aboul-Yazid, Emam, Shaaban, & El-Nashar, 2015).

d. **Tread**

Rubber has good traction properties. Tread is attached with outer ring of NPT to deliver desired traction to NPT during rolling.

1.2.2 **Working Principle**

Body of NPT deforms at the contact area when center of hub is loaded. Flexible spokes deform and buckle under applied load. Resultantly straightening of the composite ring at contact area happens which develops the contact patch. Spokes which are not related to contact area remain in tension. Buckling of spokes under application of the load is given in Figure 1.2.

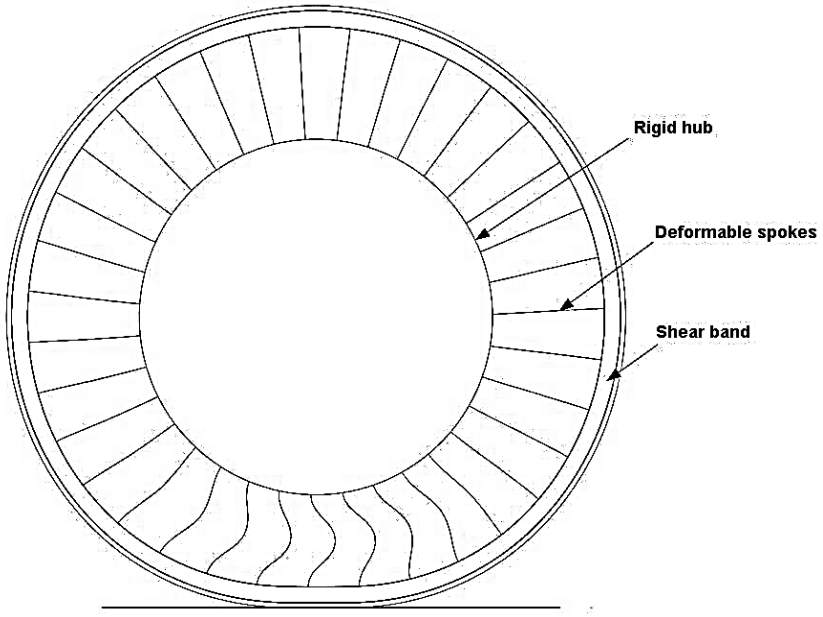

Figure 1.2: Deformation of NPT under vertical load

(Rhyne & Cron, 2006)

1.3 Cornering Characteristics

Tire properties effect handling, directional stability, ride, safety and comfort of the vehicle. Evaluation of tire performance is necessary for handling, stability and safety assessment of a vehicle, specially the military vehicles which confront extreme terrain and operational challenges. Therefore, a NPT must be evaluated for its static and dynamic performance. Cornering characteristics of tire play a significant role in studies of vehicle dynamics. Steady state cornering properties of tire provide basis for study on cornering with braking, driving and non-steady state cornering behavior of tires. Different theoretical and empirical models were presented by researchers to investigate the cornering properties of tire under steady state conditions. However, these require extensive experiments to determine the parameters required for application of these models. Apart from field testing of tires, a number of tire testing setups were developed by the developers to determine static and dynamic response of tires. However, such equipment is costly, requiring skilled staff with longer testing durations to extract desired data. Certain limiting loads and field tests cannot be applied during these tests. Repetition of these tests for verification is also another point of concern. Researchers tried to find out different alternatives to overcome these limitations.

Fortunately, recent computer technology provides us the opportunity to perform most of the laboratory tests of tires through modeling and simulation using an array of software by producing comparable results. Even the tire tests involving limiting conditions of high speed and loading can also be simulated. Finite element modeling and analysis of tires is difficult due to involving different materials with varying properties, however it is multipurpose in its applications (Chae, 2006). In this study, cornering characteristics of a NPT with hexagonal lattice spokes are investigated using a finite element commercial code ABAQUS. Cornering characteristics of NPT are compared with a similar PT. Effect of NPT on handling and stability of vehicle is also studied using a vehicle dynamics software CARSIM.

1.4 Thesis Layout

In chapter 1, potential advantages of non-pneumatic tires, their structure and working principle is discussed. Cornering characteristics and use of FEM to find cornering characteristics is also briefly introduced.

In chapter 2, literature review encompassing types of NPTs, tire characteristics, steady state cornering and tire modeling methods is given. In this chapter details about finite

element modeling of NPT, handling & stability of vehicle and testing procedures are also focused. In last part of the chapter review of dedicated research on static and dynamic behavior of NPTs is deliberated.

In chapter 3, details about geometric, structural and material modeling of NPT with hexagonal lattice spokes, used in ABAQUS, are discussed. Specifics of meshing, boundary conditions and load application are also described.

In chapter 4, results of static and steady state cornering behavior of NPT are described and discussed. Outcomes of vehicle test procedures of double lane change and fishhook procedures under different working conditions are also discussed while comparing NPTs with PTs.

In chapter 5, brief conclusions from results and discussion are narrated with recommendations for future work.

CHAPTER 2: LITERATURE REVIEW

In this Chapter, types of NPTs are described and tire force & moment characteristics are explained. Cornering characteristics of tires and available tire models to study tire cornering characteristics have been studied. Moreover, vehicle handling and testing procedures are also briefly discussed.

2.1 Types of NPT

A general NPT design has been defined in introduction part of this thesis. One of the most important components of a NPT is its spokes which replace the air of a pneumatic tire. NPTs can be divided into certain types according to structure of tire. Following are most common types of NPTs (Figure 2.1) described in literature (Zhang, Lv, Song, Guo, & Gao, 2013): -

a. PU solid filled
b. Tread with plate spokes
c. Non-plate spokes
d. NPT with Net type tread

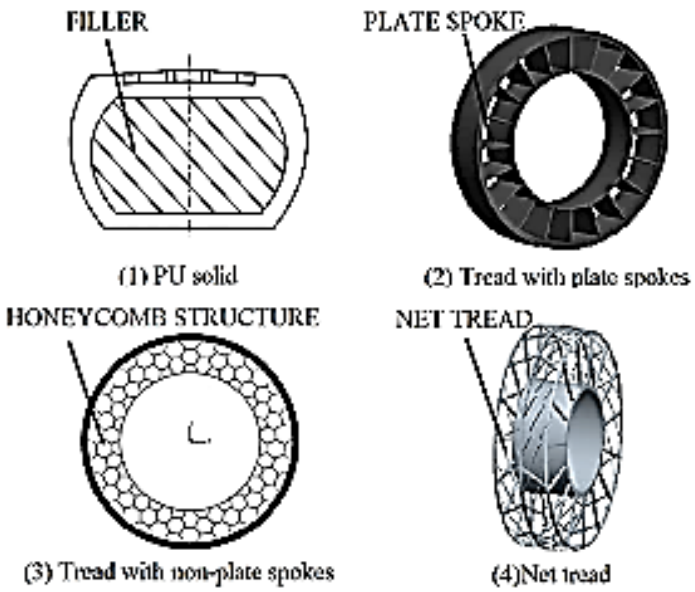

Figure 2.1: Types of NPTs

(Zhang et al., 2013)

Each structural design is having its own pros and cons, however most of the published research is available related to the plate spoke type structure and the tread with non-plate spokes. NPTs with hexagonal lattice spokes have been selected for the study.

2.2 NPT with Hexagonal Lattice Spokes

Efforts were made by tire engineers to replace air in pneumatic tire with cellular structures in NPTs. Cellular lattice(honeycombs) are periodic microstructures made of cellular materials. Cellular lattice is strong, having high out of plane stiffness in longitudinal direction of cells. However, the lattice is more compliant, about three times, when considered for in plane directions. Out of plane properties of cellular lattice has been widely used in light weight applications where strength of materials is required. Generally, these applications include placing these structures as a sandwich between other materials for giving them strength, while maintaining lower weight. Weakness of in plane properties limited their use in different structures. Recently, higher in plane compliance properties of hexagonal lattice spokes are focused by researchers for structures requiring light weight and high compliance.

Initial studies were conducted by engineers for effective Poisson's ratio and the moduli basing on property of structures dominated by bending. In plane properties including effective moduli and yield strengths of different cellular shapes including triangular, square, diamond and hexagonal shapes were investigated. Following was the outcome of these studies:

a. Cellular lattice having diamond and triangular cells are found to be appropriate for design applications which require high modulus.

b. Lattice with hexagonal and square cells are more suitable for fatigue resistant cellular design. Since the spokes of a NPT undergo repeated cycles of high tension and compression, therefore these types of lattice were found more suitable for use in NPTs(Jaehyung Ju, Kim, & Kim, 2012).

In plane properties, like strength and stiffness, of hexagonal lattice can be tuned to the requirement of NPTs by changing lengths of their sides, angle of cells and thickness of sides(Jin et al., 2018). Considering a hexagonal cell, it has four in-plane elastic constants which are independent of each other. These include two Young's moduli in each axis direction, shear modulus and Poisson's ratio. Elastic behavior of hexagonal cells is modelled by the researchers using the standard formulae of beams. Developments for calculation of the effective moduli are called the theory of cellular materials. Effective moduli under cellular material theory are described as under(Gibson, Ashby, Schajer, & Robertson, 1982): -

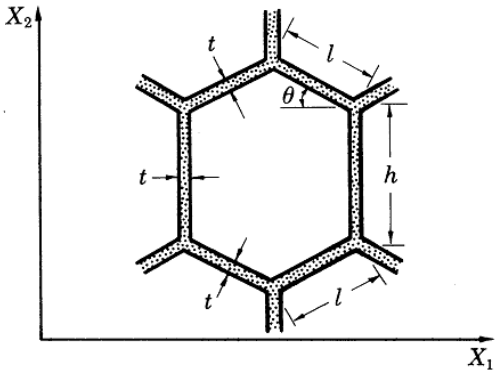

Figure 2.2: Structure of a hexagonal cell

(Gibson et al., 1982)

$$E_r^* = E_S \left(\frac{t}{l}\right)^3 \frac{\cos\theta}{\left(\frac{h}{l} + \sin\theta\right).\sin^2\theta} \tag{2.1}$$

$$E_\Omega^* = E_S \left(\frac{t}{l}\right)^3 \frac{\left(\frac{h}{l} + \sin\theta\right)}{\cos^3\theta} \tag{2.2}$$

$$G_{r\Omega}^* = E_S \left(\frac{t}{l}\right)^3 \frac{\left(\frac{h}{l} + \sin\theta\right)}{\left(\frac{h}{l}\right)^2\left(1+\frac{2h}{l}\right)\cos\theta} \tag{2.3}$$

Where E_S is Young's modulus of constitutive material and E_r^*, E_Ω^*, and $G_{r\Omega}^*$ denote the effective modulus in radial, effective modulus in circumferential, and effective modulus in shear directions, respectively. t is the thickness of the cell wall while l , θ and h represent average values of cell inclined lengths , cell angles and vertical cell lengths of lattice respectively (Figure 2.2). Density of lattice is given by following relationship: -

$$\rho^* = \rho_s \frac{t/l\left(\frac{h}{l}+2\right)}{2\cos\theta\left(\frac{h}{l}+\sin\theta\right)} \tag{2.4}$$

Where ρ^* is density of hexagonal lattice and ρ_s represent density of constituent material(Balawi & Abot, 2008; Jaehyung Ju et al., 2012).

2.3 Tire Characteristics

Tires transfers forces & moments from road to vehicle which greatly affects dynamics including handling and stability of the vehicle. Ideal rigid wheels make contact with the

ground at a single point, however the compliant tires (PT and NPT) deform under vertical load of vehicle and make contact with ground at an area known as footprint. This footprint area is called tire contact patch. Figure 2.3 shows the contact patch of a pneumatic tire under loading.

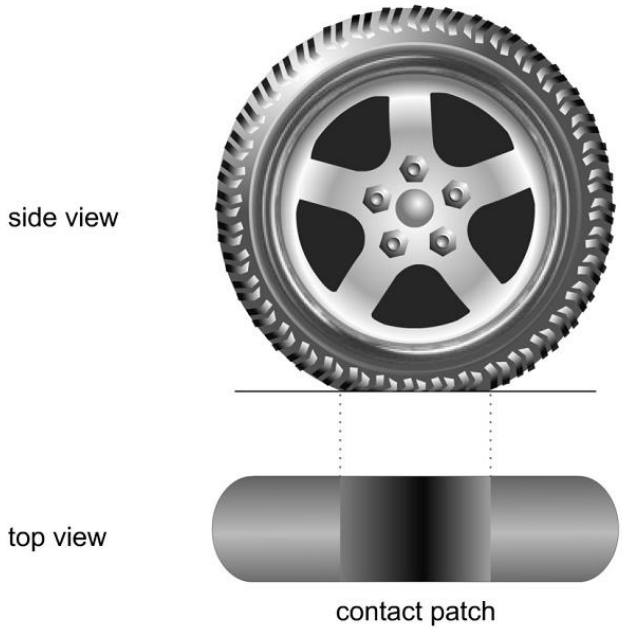

Figure 2.3: Tire contact patch

(Rajesh Rajamani, 2006)

Forces and moments acting during operation of tire are given in Figure 2.4. Tire axis is taken from center of the contact patch. Crossing of ground plane with plane of tire defines the X axis. X axis is also known as the longitudinal axis. Axis perpendicular to the ground pointing downwards is the Z axis. Axis pointing rightwards is Y axis which is lateral axis of the tire. It is assumed that force from the road acts on the center of contact patch. This force can be disintegrated along already stated axes. Force *Fx* acting along the X axis is named the longitudinal force. Force *Fy* acting along the *Y* axis represent the lateral force, and the vertical force *Fz* acting along the Z axis is vertical force. In the same way, the moments acting on tire from road are distributed along three axes. Moments along X, Y and Z axes are *Mx, My* and *Mz* respectively. *Mx, My* and *Mz* are termed as overturning moment, rolling resistance moment and aligning moment correspondingly.

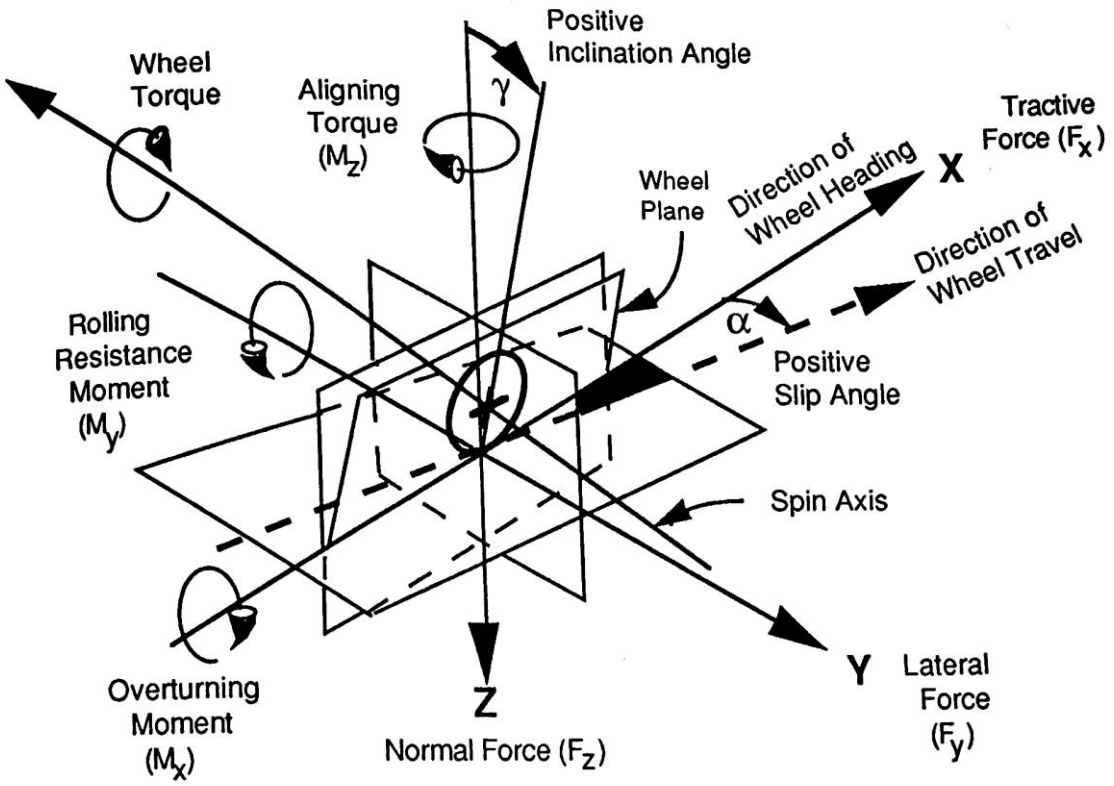

Figure 2.4: SAE tire axis system

(Gillespie, 1992)

Camber of tire γ is not being considered in this thesis due for simplification and clarity in understanding. This research is primarily related to the lateral force *Fy* and the aligning moment *Mz*. The tire pull phenomenon may occur when these tire characteristics act at a distance with respect to their origin. Lateral force affects linear handling & stability of vehicles. Handling & stability properties of automobiles at high accelerations are governed by nonlinear portion of the lateral force. Lateral force curves are dependent on the vertical loads on tires and slip angles (Pacejka, 2012; Rajesh Rajamani, 2006; Wong, 2008). This dependency is discussed in subsequent paras.

2.4 Cornering of Tires

Non-zero slip angle is produced on steering of a vehicle from its straight positon of movement. Inertia of vehicle and the traction of tire produce deflection in lateral direction of contact patch. At this point the longitudinal axis X of tire does not coincide with longitudinal axis of road due to tire properties. An angle exists between these two longitudinal axis. This angle is known as slip angle and behavior of tire is known as cornering behavior (Figure 2.5). Deflection of tire increases from front portion of the

contact patch to the rear. It reaches at maximum value when traction force becomes equal to elastic force at that point. Due to saturation at that point, tread starts to slide back to its original position. Asymmetry of developed lateral force causes resulting force to position at rear side of contact patch at a distance known as the pneumatic trail (Gillespie, 1992).

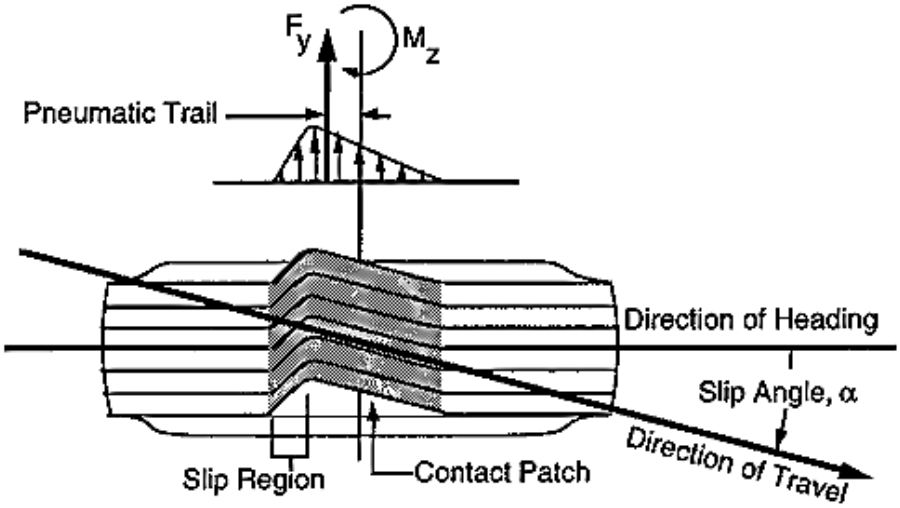

Figure 2.5: Deformation of rolling tire by lateral force

(Gillespie, 1992)

During cornering the ratio of lateral velocity and longitudinal velocity is called lateral wheel slip. It is tangent of slip angle with negative sign. Negative sign is chosen to keep lateral force positive with positive slip angle.

$$\tan \alpha = -\frac{V_y}{V_x} \tag{2.5}$$

Force *Fy* and aligning moment *Mz* are produced as a result of given slip(Figure 2.6). These are functions of vertical load and constituents of slip. These tire characteristics for steady-state motions (pure slips) can be shown in general as under: -

$$F_x = F_x(k, F_z), \quad F_y = F_y(\alpha, F_z), \quad M_z = M_y(\alpha, F_z) \tag{2.6}$$

k is longitudinal slip in equation 2.6. Wheel vertical force or load *Fz*, calculated from tire vertical deflection, may be taken as a given quantity (Pacejka, 2012).

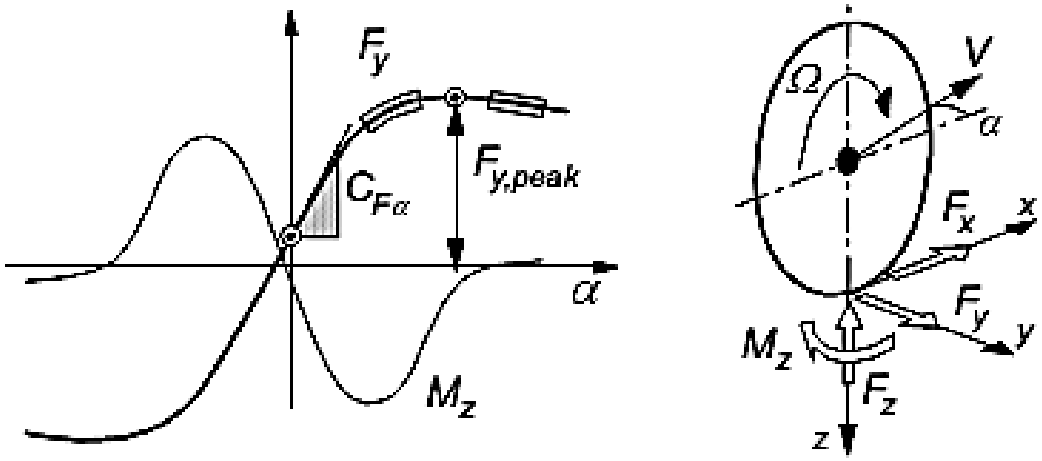

Figure 2.6: Characteristic shapes of lateral force and aligning moment during cornering

(Pacejka, 2012)

Pure slip is defined as a condition when either of the slip arises in separation. When there is no pure slip then both lateral and longitudinal forces arise. This condition is termed as a combined slip. Explanation of reduction in force in combined slip lies in the friction circle(Figure 2.7). Lateral or longitudinal force drops when other slip component is included. If braking or acceleration is designed during cornering, then lateral force is affected by generated longitudinal force. As per law of friction, lateral force and longitudinal force must fulfill following equation:

$$\sqrt{F_x^2 + F_y^2} \leq \mu Fz \tag{2.7}$$

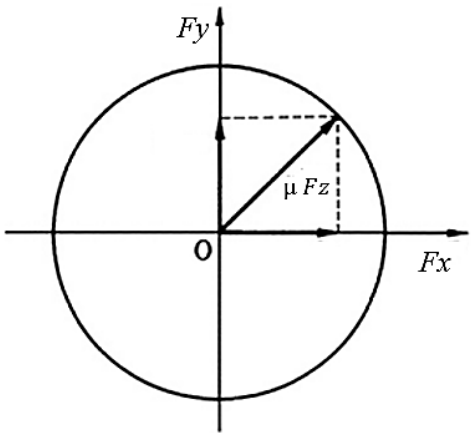

Figure 2.7: Description of friction circle

(Abe, 2015)

Equation 2.7 states that forces acting in contact plane of the tire cannot be more than maximum force determined by product of vertical load of tire and friction coefficient. Thus resultant force is restricted inside the circular region having radius equal to μ times the vertical load *Fz* of tire. The circle so formed is known as friction circle. Thus if there exist a longitudinal force caused by traction or braking then maximum lateral force will be decreased accordingly. Maximum lateral force in that case will be given by equation 2.8. In steady state cornering conditions, longitudinal force is negligible therefore maximum lateral force is equal to μFz (Abe, 2015).

$$Fy = \sqrt{\mu^2 F_z^2 - F_x^2} \tag{2.8}$$

It is clear from the above discussion of friction circle that horizontal and lateral frictional forces cannot be more than a maximum value (i.e. radius of 'friction circle'). Slopes of lateral and longitudinal curves plotted against slip angle and slip ratios represent longitudinal & lateral slip stiffness, respectively. Stiffness of longitudinal slip is represented by C_{F_k} while cornering stiffness is designated by C_{F_α}. Cornering stiffness is a very important property parameter of tire which directly effects vehicle handling and stability. Aligning stiffness, represented by C_{M_α} is negative of slope of aligning moment and slip angle plot (Figure 2.6) at zero slip angle. Force & moment characteristics are linear at very small slip. These characteristics can be denoted by following relationship in linear region (Pacejka, 2012):

$$F_y = C_{F_k} k \tag{2.9}$$

$$F_y = C_{F_\alpha} \alpha \tag{2.10}$$

$$M_z = -C_{M_\alpha} \alpha \tag{2.11}$$

It is highlighted that effect of camber is not included in these relationships. Above mentioned relationship equations have been formulated in such a manner such that all the coefficients in these equations materialize as positive quantities. Typical value of cornering stiffness has been found to be 50 % lesser than the longitudinal slip stiffness in PTs (Pacejka, 2012). Cornering stiffness is also known as the cornering coefficient. Cornering force of a PT can be estimated by linear function of slip angle at small values (till 2° of slip angle for light vehicles) with proportionality constant of cornering stiffness. However, the linear model has a drawback that when slip angle exceeds from certain value then

behavior of lateral force cannot be determined by this relationship. Tire lateral force cannot exceed the product of vertical force and coefficient of friction between road and tire. Therefore it is necessary to use nonlinear model to ascertain lateral force behavior at high slip angles(Tönük & Ünlüsoy, 2001).

2.4.1 **Steady State Cornering**

Tire moving under zero horizontal force in a straight ahead position is in a steady state condition. However, during cornering this balance is disturbed and there becomes a transfer phase between pre cornering and cornering steady states. During this phase tire generates lateral deflection to attain steady state force condition. Researchers have learnt that it takes almost half and one revolution of tire to reach steady state condition during cornering (Zhou, Yang, Gao, & An, 2017).

2.5 **Tire Modelling Methods**

Tire is a complex structure comprising of different components. Various tire modeling methods have been developed to investigate tire mechanical properties to bring improvement in overall performance of tires. Selection of these models is based on the aim of research for example few models are good in describing static and dynamic behaviors of tire while others are more focused on characteristics of vibration, noise and harshness. If we go a bit further in detail, then it highlights that even from first category few are good in describing steady state while others well describe the transient dynamic behavior of tire. Similar is the case with tire characteristics' description models for pure and combined slips. Most of these models are specific to the aim of research. Although some of tire modelling approaches have become more popular and matured over time like FTire, SWIFT, Magic Formula and brush tire models, there is still work required to get real dynamic response of tire. In following paras, a brief introduction of these tire models is given followed by a detailed literature survey on finite element method which has been used as a main tire analysis tool in this thesis. There are different classifications for tire models in literature. However, three distinct tire models exist in literature for tire cornering simulations.

2.5.1 **Analytical Models**

Analytical tire models are used to obtain behavior of tires under various static and dynamic conditions. Analytical models are formulated on physical phenomenon occurring in tire structure and tire contact patch. These use very few equations and a lot of simplifications to represent tire behavior. These simplifications add to the inaccuracies represented in

results of their outcome. Although they have simplification and inaccuracies however they are very useful in providing basic knowledge of tire behavior. These models usually use very few equations in explicit form, that is, iterative solutions are usually not required for their solution. Due to simplicity these models were considered more suitable to integrate with overall vehicle system models to study vehicle dynamics. Though analytical tire models may not be able to represent and explain all the behaviors of tires, however, their parameters have a certain significance. Most famous example of analytical tire model is brush tire model. These models are more significant when modeling of tire is integrated with complex system. These systems may include driving simulators or dynamic models of vehicles.

2.5.2 **Empirical Models**

These tire models were developed to compensate the inaccuracies caused by simplification in analytical tire models. Empirical tire models are constructed basing on results obtained through experiments. These tire models follow a general tire behavior and use curve fitting methods to fix the experimental data. One of the most famous example of these tire models is magic formula model. Magic formula tire model was initially developed for steady state conditions, however later on it was further extended to the transient behavior of tires. Empirical tire models like Magic Formula tire model use a no of coefficients which can only be obtained through extensive tests. Moreover, since empirical models try to adjust functions to the test data, it is difficult to get physical knowledge and understanding of actual tire behavior.

2.5.3 **Physical Models**

These models are formulated to simulate complex physical nature of tire materials, their interface with environment and each other. These tire models are more detailed and complex among all of the tire models. Though some simplifications are made yet these models involve a large number of nonlinear equations. These tire models are usually in discretized form and require advanced numerical techniques to solve them. Finite element models are the most popular example of these models (Yang, 2011).

2.6 **Finite Element Models**

Numerical analysis has been applied in deign processes since three decades. Finite element (FE) method is one of the numerical analysis techniques that is being vastly used in tire design processes. Researchers have demonstrated that finite element method is potentially

accurate method to model the realistic tire simulations. Tönük & Ünlüsoy (2001) used finite element modeling of tire to predict cornering characteristics using finite element software MARC. They determined that FE tire model was able to predict tire cornering force characteristics with acceptable accuracy thus saving expensive procedures of development of prototype and testing. Rao & Kumar (2007) performed pneumatic tire dynamic behavior simulation using arbitrary lagrangian eulerian(ALE), explicit and implicit dynamic finite element method (Figure 2.8) and compared them with experimental results. They concluded that ALE method is more economical in computer resources for steady state simulations. Moreover, explicit method had an edge of use in transient conditions where ALE could not be used.

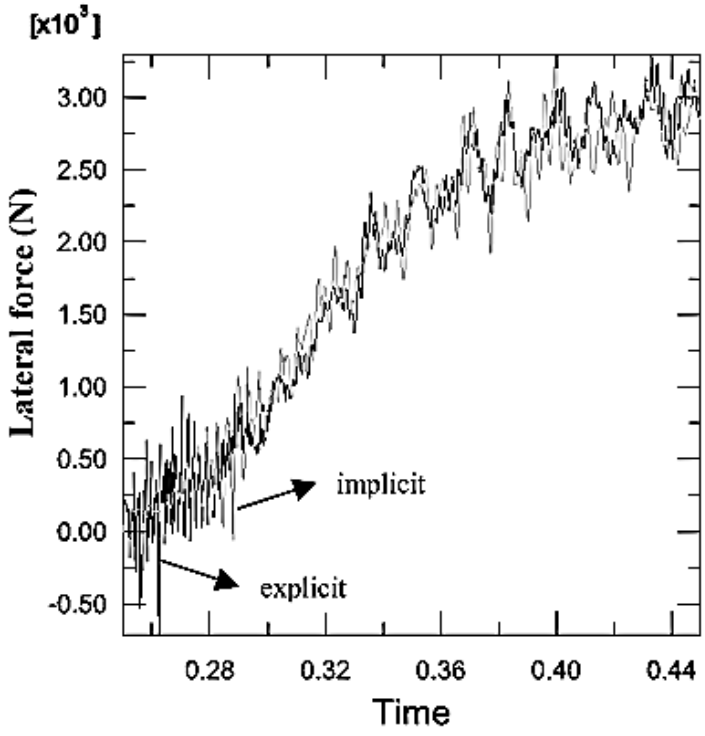

Figure 2.8: Comparison of explicit and implicit dynamic methods for tire lateral force (Rao & Kumar, 2007)

Zhou et al. (2017) adopted finite element method to examine effect of tire design, material and working conditions on cornering stiffness of PTs. They used finite element code ABAQUS / Explicit to simulate cornering behavior of tire under different slip angles and verified the results with test data. Koishi, Kabe, and Shiratori (1998) demonstrated feasibility of cornering simulation using an explicit FE code, PAM-SHOCK and concluded that FEM results coincide with the experimental test results. Kabe and Koishi (2000) performed cornering simulations of tire using ABAQUS / Explicit and ABAQUS/Implicit

(ALE) analysis and compared the results with experimental data. Both Explicit and implicit results well agreed with the experimental results, however implicit method based ALE method turned out to be more resource efficient than the explicit method. Wei and Olatunbosun (2017) predicted the influence of tire operating conditions and design parameters on cornering characteristics of tire using ABAQUS Implicit method and concluded that cornering stiffness results agree with experimental results. Deng et al. (2018) developed a finite element model of a novel non-pneumatic mechanical elastic wheel (MEW) by using finite element code ABAQUS. Basing on the results of numerical simulations and experiments, they concluded that finite element model was capable of predicting the dynamic behavior of wheel under various operating conditions with accuracy and reliability. Zhu et al. (2019) presented a finite element analysis model to investigate the cornering behaviors of mechanical elastic wheel in ABAQUS and summarized that results could reflect realistic working conditions during cornering of tire. Furthermore, the model could provide foundation to predict tire cornering behavior for different NPTs.

Various commercial finite element softwares like ANSYS and ABAQUS are being used worldwide in tire design processes. FE code ABAQUS is used in this thesis to ascertain cornering characteristics of a NPT with hexagonal lattice spokes. Finite element method works on division of whole tire structure into small elements. Desired mechanical properties are calculated on nodes of these elements. Numerical modeling of tire is a difficult task. It involves modeling of complex multi material structure and their interaction with each other and the environment. Dynamic tire modeling is a nonlinear problem(DS Simulia, 2009). It involves different types of nonlinearities faced during FE modeling. These nonlinearities can be categorized into following three categories: -

a. Material nonlinearities mostly arise due to the large deformation. Even the materials having quite a linear stress strain behavior perform non linearly under high strains.
b. Boundary nonlinearities are mostly caused by the changing boundary conditions causing the system to act nonlinearly. Contact problems are among the examples of nonlinear problems.
c. Changes in geometry during the analysis causes the geometric non linearity

2.6.1 **Finite Element Analysis for Cornering Simulation**

ABAQUS has two types of solvers which can be used to find dynamic response of tire.

These include implicit dynamic and explicit solvers.

2.6.1.1 **Dynamic Implicit Analysis**

ABAQUS implicit uses matrix inversion technique to find out solution of a problem. In linear problems this produces very good results. This analysis method can also be used effectively for smooth nonlinear problems. Implicit analysis in ABAQUS uses Newton iterative method. Dynamic equilibrium is satisfied at end of each time increment. Solutions of the implicit analysis are unconditionally stable and can permit larger time steps. However, if model contains certain discontinuities like making breaking of the contact then the achieved convergence is lost causing a large number of iterations to reach to solution. Though implicit dynamic analysis can be used for rolling and cornering of tires, yet it is not often used by researcher. Implicit dynamic analysis requires very small time steps to analyze dynamic behavior. It is also not efficient to solve changing contact conditions of rolling tires. Newtonian iterations cause excessive burden on computational resources and at times it is difficult to get solution.

2.6.1.2 **Explicit Analysis**

Explicit direct integration process is used to solve the dynamic response in explicit analysis. Explicit integration method is used to solve dynamic problems. Calculations of velocities and displacements are made in relations of the quantities which are given in start of an increment. In this method matrix inversion or iterations are not required which is an advantage over implicit method. This however requires a small step time, depending on highest frequency calculation of model. Owing to these limitations this analysis can take longer time period for reaching a steady state condition. This analysis is best suited for transient behavior simulation of tires where small time intervals are involved. Though this analysis method has been used by many researchers for cornering behavior simulation yet they have restricted to small range of slip angles. There is also a great possibility of accumulation of error due to involvement of a huge no of integration steps in steady state analysis(DS Simulia, 2009).

2.7 **Vehicle Handling and Stability**

Tire characteristics affect handling and stability of a vehicle. Before going into detail of these effects, a short introduction to vehicle handling and stability is given.

2.7.1 **Handling**

Handling is a roughly used term. Vehicle handling indicate response of a vehicle to input given by driver. Behavior of vehicle during driving depend on many factors including assessment of the condition and decision making by the driver, so it will not be fair to wholly attribute handling characteristics towards the vehicle. Thus handling is measure of combination of both vehicle and driver (Gillespie, 1992). Various types of maneuvers are possible under different road and environmental conditions confronted by combination of man and vehicle. Maneuvers also depend on the circumstances confronted. These may be normal handling where a driver deliberately makes a maneuver, or emergency handling where driver may tend to avoid trouble or remain out of further trouble. Vehicle characteristics can be favorable in normal handling or emergency handling or in both conditions (Gillespie, 1992; Versace & Forbes, 1968).

2.7.2 **Stability**

Directional stability of a vehicle is its ability to follow a given path by avoiding skidding. It is one of the important characteristics of lateral dynamics of the ground vehicles. Tires determine interaction of vehicle with road including variation of different forces and moments acting between them. Mechanical properties of tires are the defining factor in these interactions affecting forces and moments. Ability of a vehicle to avoid turnover under specific lateral accelerations is known as lateral stability. Apart from driver factor, safety of a given vehicle largely depends on lateral and rollover stability under normal and most importantly the emergency conditions (Cao, Jing, Guo, Engineering, & 2013, 2013; Celeri & Chiesa, 1974).

2.7.3 **Effects of Tire Characteristics on Handling and Stability of Vehicles**

Lateral stability of a vehicle can be affected by cornering stiffness, compliance properties and coefficient of friction of tires. Vehicle ride also depends on tires. Since handling, ride and stability of vehicle are interconnected, so there is always a tradeoff between desirable handling and ride while maintaining the stability of vehicle. Analysis of different tires show that tire size and aspect ratio dominate tire characteristics. Thus selection of tire becomes more important for vehicles with minimal stability problems. Testing under sensitive transient maneuvers can make the finalization of tires for a specific vehicle (Allen, Myers, Rosenthal, & Klyde, 2000). Thus specific maneuvers were searched for which NPT can be tested for their effect on handling and stability of vehicle.

2.8 Vehicle Testing Procedures

“International organization of standardization” (ISO) and “National highway traffic safety administration” (NHTSA) of USA are two renowned organizations that have extensively worked on standardization of handling and stability test procedures. ISO has issued the standard ISO-3888 which gives details of testing of a vehicle through double lane change maneuver. Different test parameters are defined in the standard. NHTSA has extensively worked to finalize the rollover stability maneuver for vehicles. Under its new car assessment program (NCAP), NHTSA conducted experimental assessment of different rollover test procedures including J-Turn, fixed time fishhook, roll rate feedback fishhook and Nissan fishhook test procedures. Basing on the assessment criterion of the repeatability, objectivity, discriminatory capability, perform ability and reality appearance they assessed the procedures (Forkenbrock, Garrott, Heitz, & O’Harra, 2003b). In this thesis fixed timing fishhook procedure is used to compare vehicle performance with pneumatic and non-pneumatic tires. Double lane change and fishhook procedures will be briefly described in following paras.

2.8.1 Double Lane Change (DLC) Procedure

ISO designed double lane change procedure (Figure 2.9) is maneuver of obstacle avoidance by a driver. In this maneuvers a driver changes lane to avoid an obstacle then shifts to second lane, establish there and then return back to the original lane. This maneuver is developed to test vehicle response to input given by driver during emergency conditions. Apart from vehicle properties the maneuver also depends on driving skills. Driver has to engage this maneuver without displacing the cones. This procedure is closed loop test procedure (ISO, 2018). This procedure is inbuilt in commercial vehicle dynamics software CARSIM.

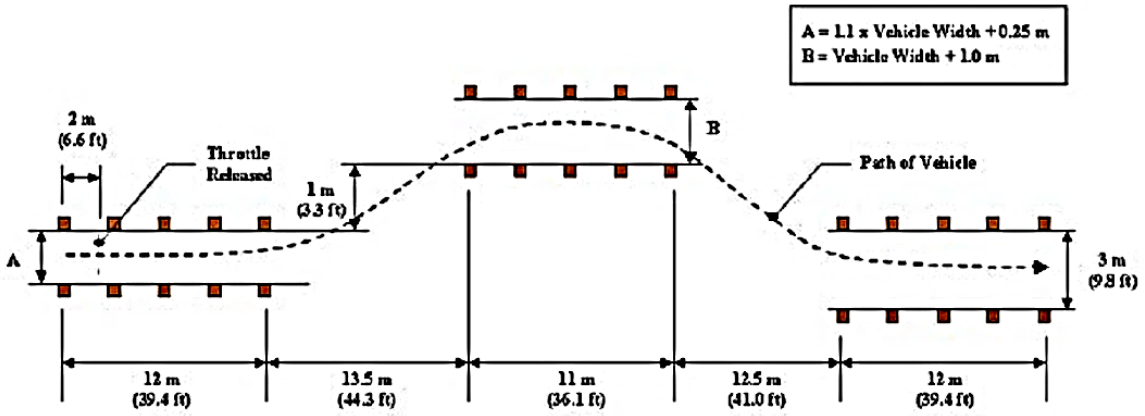

Figure 2.9: Double lane change procedure (ISO-3888)

(Forkenbrock, Garrott, Heitz, & O'Harra, 2003a)

2.8.2 **Fishhook (FH) Procedure**

Number of details have been given by NHTSA regarding loading, test preparation and condition of vehicle assemblies like tires etc. used in this procedure. Here only the minimum required information is described in order to understand the procedure. Main test procedure is given in brief form and other supplemental test procedures are not discussed as the same are described in detail in the relevant documentation. Fishhook test procedure can be distributed into two main test maneuvers. First maneuver is characterization maneuver while the second one is rollover resistance (fishhook) maneuver.

2.8.2.1 **Slowly Increasing Steer (SIS)**

The tests start with initial maneuver known as slowly increasing steer maneuver. Lateral dynamics of the vehicle are characterized through SIS maneuver. Each vehicle is characterized to find out steering handwheel angle at which it produces 0.3g of lateral acceleration at a given constant speed. This steering handwheel angle is then used as an input for main fishhook maneuver.

2.8.2.2 **NHTSA Fixed Timing Fishhook Maneuver**

Once the steering hand wheel position for the given speed of a vehicle is calculated then this maneuver is performed. The vehicle is driven straight on road. When vehicle reaches at a little higher speed than the required test speed then driver releases throttle and performs a series of operations given in Figure 2.10, through a programmable steering machine. Initially the steering wheel is turned left with an angular speed of 720 degrees / sec for the hand wheel till it reaches 6.5 times the steering handwheel angle obtained through SIS

procedure. After the steering handwheel has completed the angle of 6.5 times the SIS steering, 250 milliseconds dwell is given after which reverse steering is performed at the same rate. Reverse steering is completed till steering angle has completed double the original steering input. After the counter steer the steering wheel position is maintained for three seconds after that it is returned to zero in two seconds. Maneuver is completed in two sequence of operations. In first sequence steering hand wheel is turned from left to right and results are obtained while in second sequence steering hand wheel is turned from right to left and results are measured.

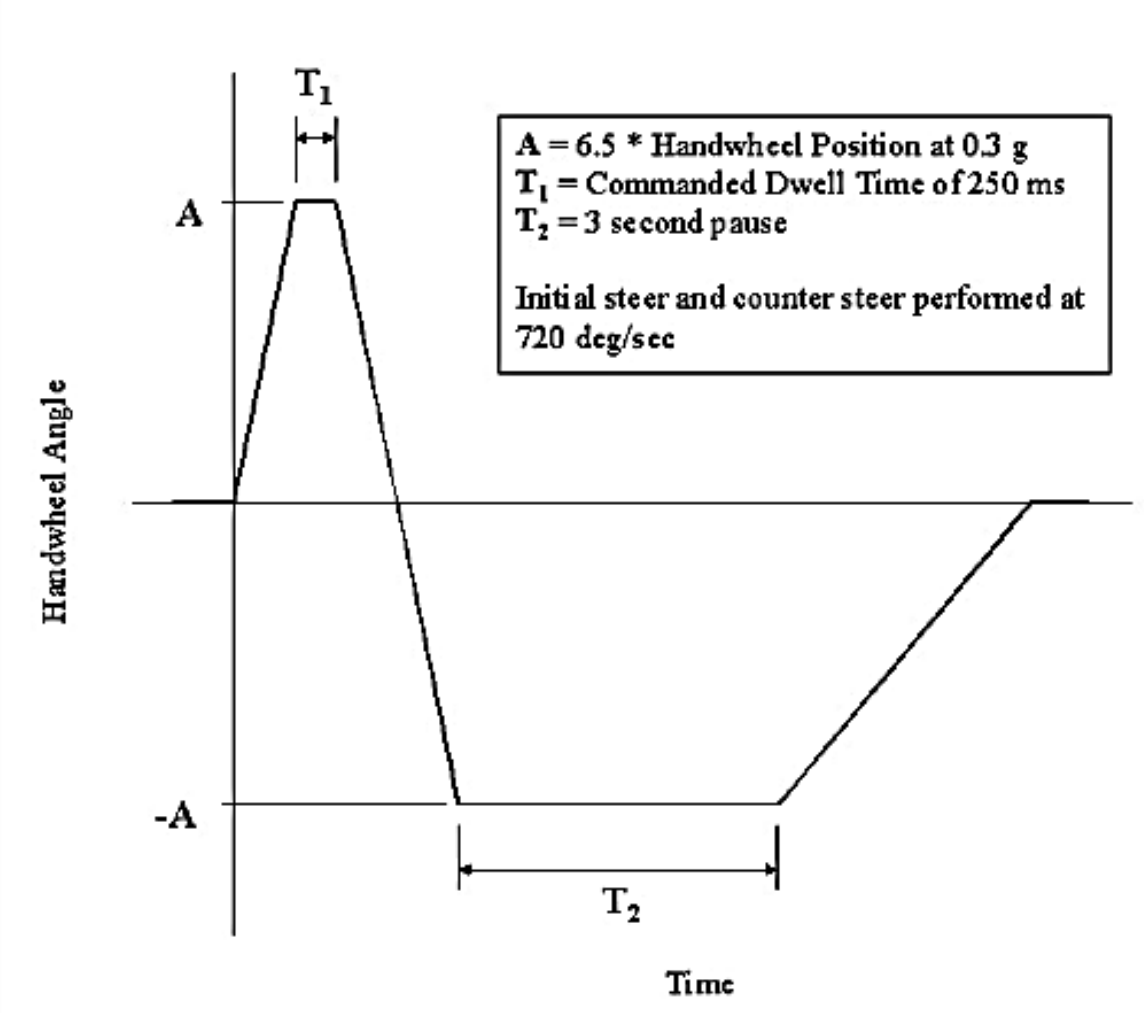

Figure 2.10: NHTSA fishhook maneuver

(NHTSA, 2013)

2.8.2.3 **Termination and Conclusion Conditions**

Test is performed from lower speed to higher speed. Minimum speed is kept as 35 mph

(miles per hour). If maneuver produces two-wheel lift at lower speeds, then tests are terminated and results are noted. Definition of wheel lift is that if wheel raises two inches from ground then it is considered as wheel lift, Wheel lift is measured through instrumentation installed on the vehicle. If test procedure doesn't produce wheel lift, then speed of test is increased and tests are repeated. Finally, test is executed at 50 mph test speed. Tests are terminated with noting the test measurements in results. A test sequence is considered complete if the vehicle encounters maneuver with maximum speed of 50 mph without two-wheel lift (NHTSA, 2013).

2.9 Previous Work on NPTs

Pajtas (1990) published a review on testing and development history of polyurethane (PU) based NPTs. It was reviewed that replacement of pneumatic tires had been wanted by the researchers since early 1900s. Number of designs were presented but none could meet the required durability and ride quality of a pneumatic tire. In this work, modeling and experimental testing of a PU based non pneumatic spare tire was performed. Basing on the comparison it was found that use of FEA tools to model NPT could be a good substitute to develop real world NPTs. Zhang et al. (2013) carried out classification of NPTs on the basis of structure. It was stated that although the research on polyurethane based non-pneumatic tires was started earlier yet the companies had started investing into that recently. Three improvement measures were suggested in NPTs for their real time application in vehicles. Those included, improving structural design and optimization of tire performance, simplification of assembly process of NPT to reduce their cost and strengthening their ability to exclude foreign materials stuck into body. Aboul-Yazid et al. (2015) numerically investigated effect of spoke structure and shear band on stress, mass, rolling resistance and normal stiffness of NPTs. Two cases were studied. First case included all types with shear layer while second study included tires without shear layer and outer ring. Comparison was made between Resilient technologies honeycomb, Michelin Tweel having spoke pairs, Bridgestone spoke pair and new curved spokes designs (Figure 2.11). Basing on the results of simulations of both the cases it was concluded that spokes pair design was better for first case while the honeycomb design was better than others in second case.

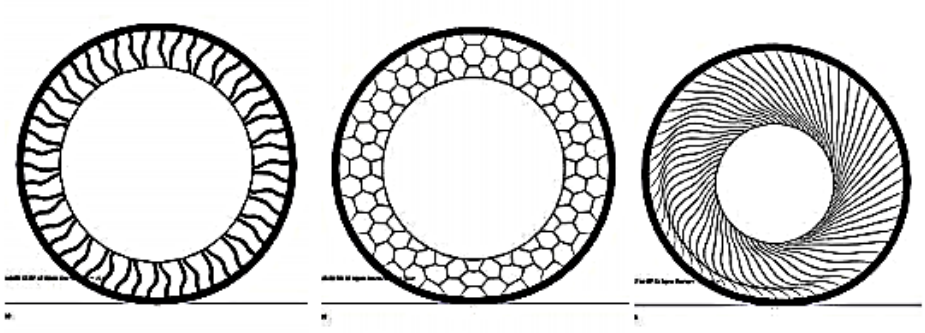

(a) Tires with shear beam

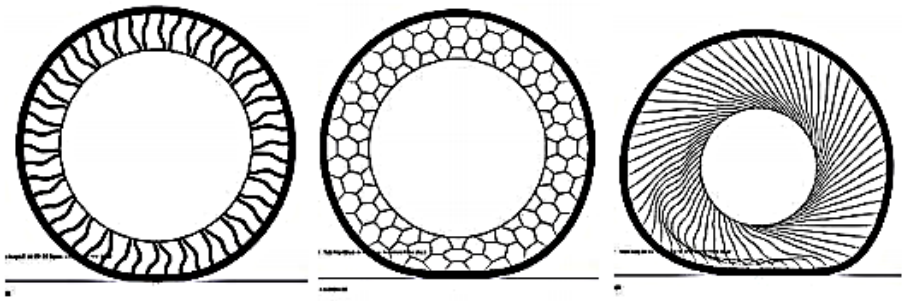

(b) Tires without shear layer and OIEM

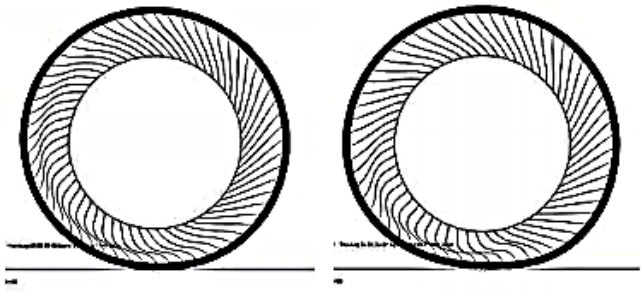

(c) New curved spoke model with shear beam (left side) and without shear layer and OIEM (right side)

Figure 2.11: Deformed shapes of compared models: a & c are with shear beam, b & c are without shear beam

(Aboul-Yazid et al., 2015)

Kim, Kim, and Ju (2013) investigated effect of vertical loading on NPT contact pressure and compared results with a pneumatic tire. Results showed that NPT vertical stiffness decreased with increase in load in contrast to the PT whose vertical stiffness increased with increase in vertical load (Figure 2.12). Decrease in vertical stiffness caused lower contact pressure. Comparison of three honeycomb tires with different cell angles revealed that hexagonal honeycomb spokes having higher cell expanding angle showed lower stresses locally.

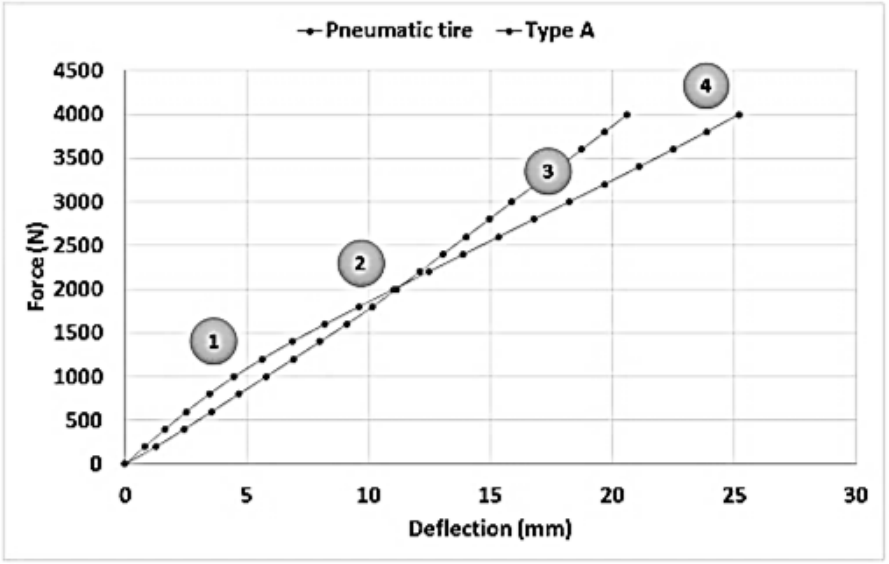

Figure 2.12: Vertical deflection of NPT (Type A)

(K. Kim et al., 2013)

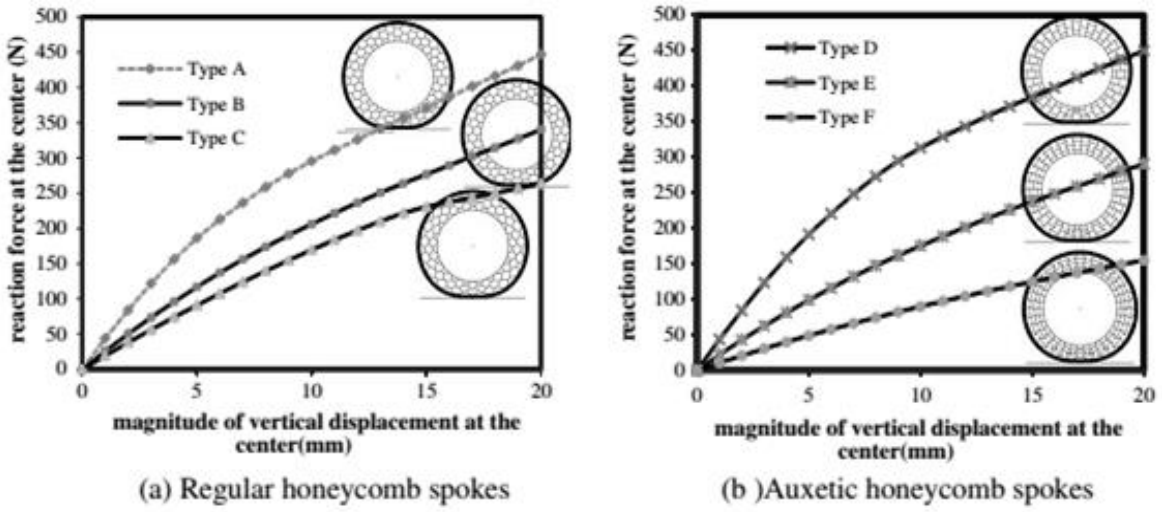

Figure 2.13: Force deflection curves of NPTs with regular and auxetic honeycomb spokes

(Jaehyung Ju et al., 2012)

Ju et al. (2012) studied flexible cellular spokes of a NPT for a design with high fatigue resistance. NPTs were designed with two different hexagonal honeycombs having equal thickness of cell wall and load bearing capacity. Flexibility of spokes increased with cell angle (Figure 2.13). Moreover, higher cell expanding angle caused lower stresses locally which lead to high fatigue resistant design. Regular and auxetic hexagonal spokes were

modeled with different cell angles and it was established that under equal load bearing capability, regular hexagonal honeycombs with a high positive cell opening angle indicated low mass and local stress than auxetic honeycomb structure.

Kim and Kim (2011) investigated change in contact pressure of NPT with change in vertical loading. Contact area of NPT was rectangular as compared to the circular contact area of PT with decrease in contact pressure (Figure 2.14). Decrease in contact pressure of NPT was caused by high lateral stiffness of tire.

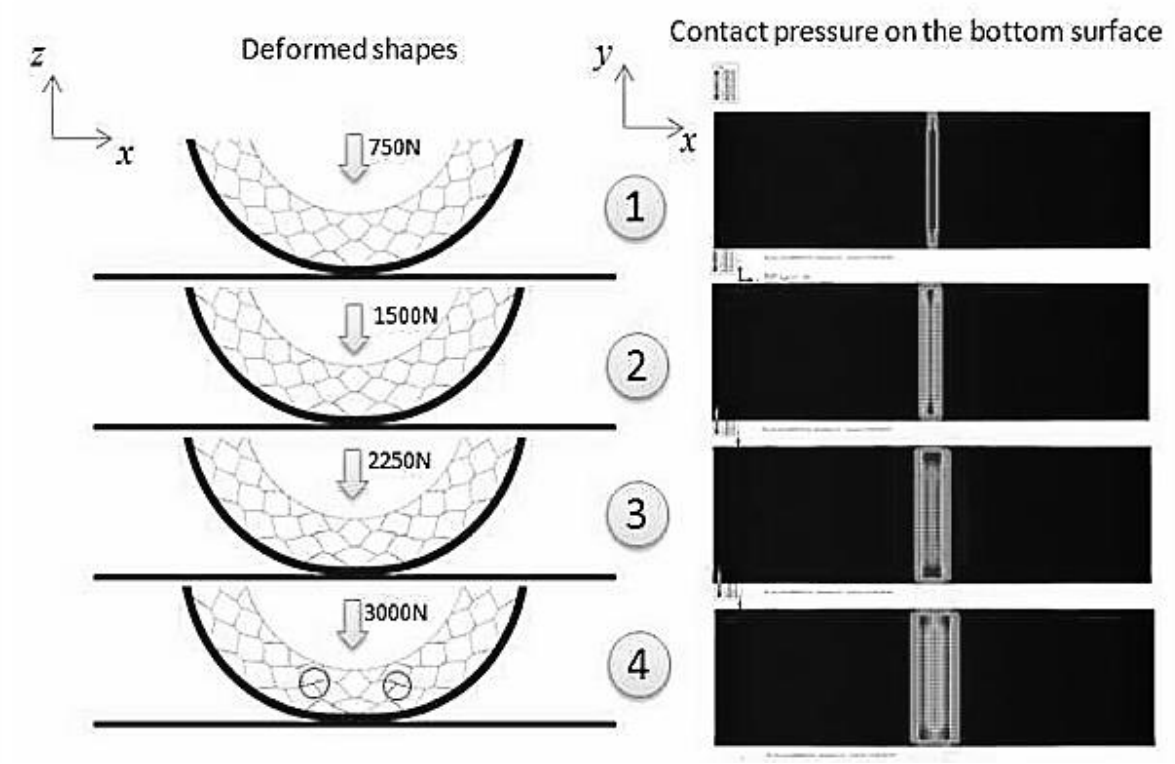

Figure 2.14: Deformation and contact pressure of a NPT

(K. Kim & Kim, 2011)

Ju et al. (2013) worked on reduction of NPT rolling resistance by using porous elastomer composite shear band instead of a continuous shear band (Figure 2.15). Results indicated that due to lesser viscoelastic energy loss, composite porous shear band reinforced with fiber could lead to fuel efficient NPT designs to save energy.

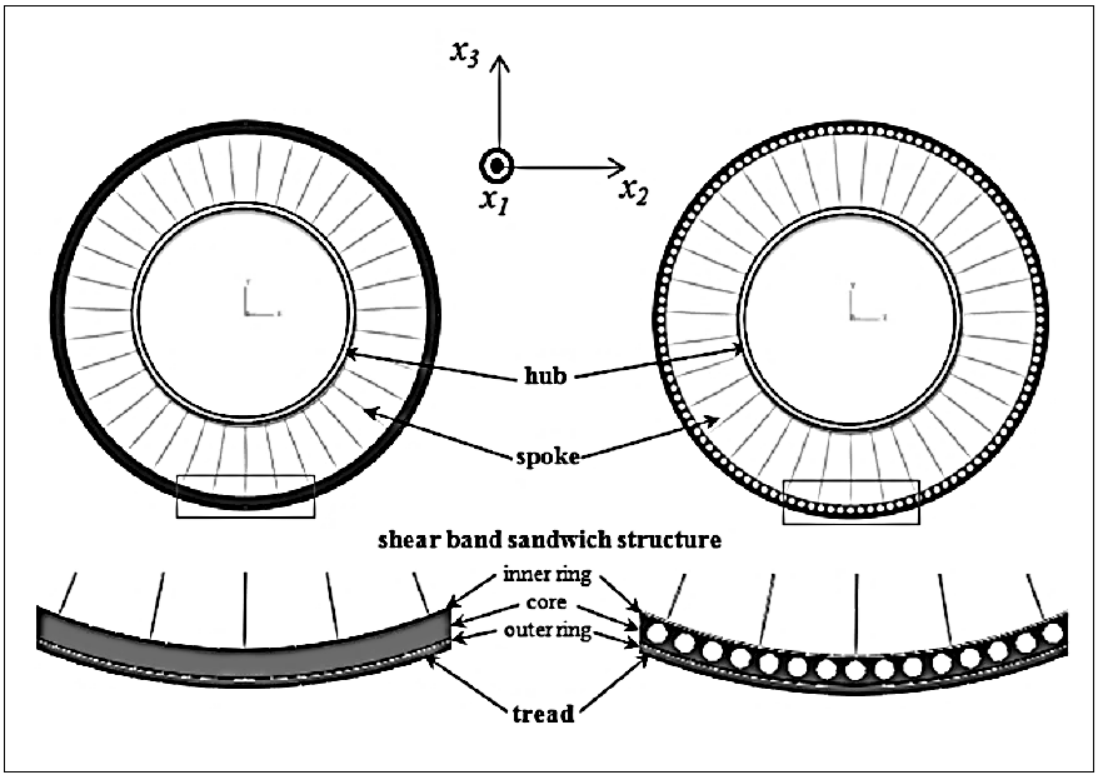

Figure 2.15: Structure of NPTs

(J Ju et al., 2013)

Veeramurthy et al. (2014) carried out study for assessing the effects of PU shear modulus, shear layer thickness and spokes thickness on rolling resistance of a NPT with single spokes structure. Numerical simulations in finite element commercial software ABAQUS were performed by using hyper and viscoelastic material models. It was concluded that increasing shear modulus of PU lowered the rolling resistance. Similar was the effect of increase in the thickness of shear band (Figure 2.16 and 2.17). The behavior was due to lesser deformation of material in those cases. Shear modulus had a substantial effect on contact pressure, rolling resistance & contact pressure. However, it was highlighted that in case of increase in thickness or shear modulus of shear band, spokes thickness was also required to be deceased to satisfy conditions of contact pressure and vertical stiffness.

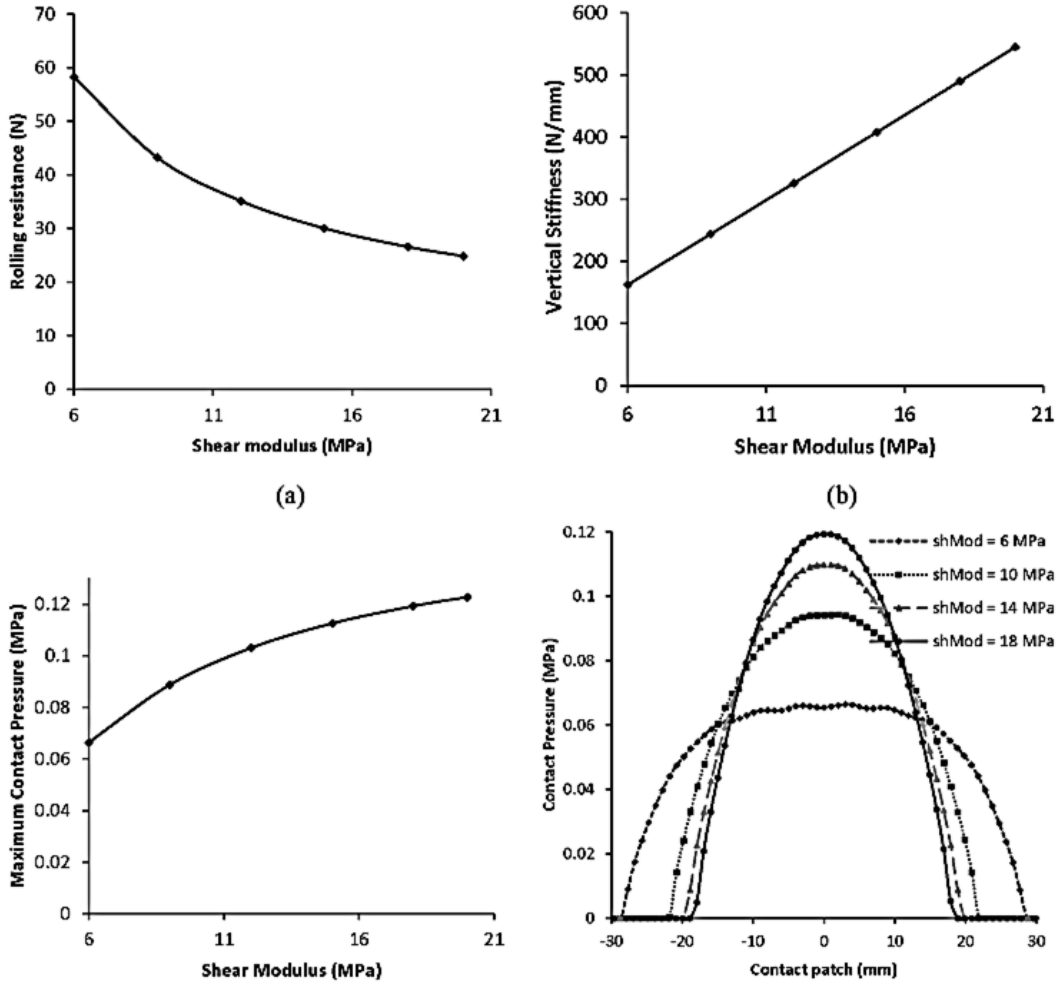

Figure 2.16: Effect of change in shear modulus on NPT behavior

(Veeramurthy et al., 2014)

Kim et al. (2015) carried out optimization of a NPT with reentrant type hexagonal lattice spokes to reduce its rolling resistance. In the study, thickness of shear band, thickness of spokes and cell angle were used as design variables. Finite element simulations were carried out by hyper viscoelastic modeling of the material. In parametric studies, it was found that by increasing the thickness of shear band and spokes, stiffness of tire increases while increase in cell angle had opposite effects on tire behavior. In sensitivity analysis, spoke thickness was found to be the most important design parameter. Optimization resulted in 15 percent reduction in rolling resistance of tire.

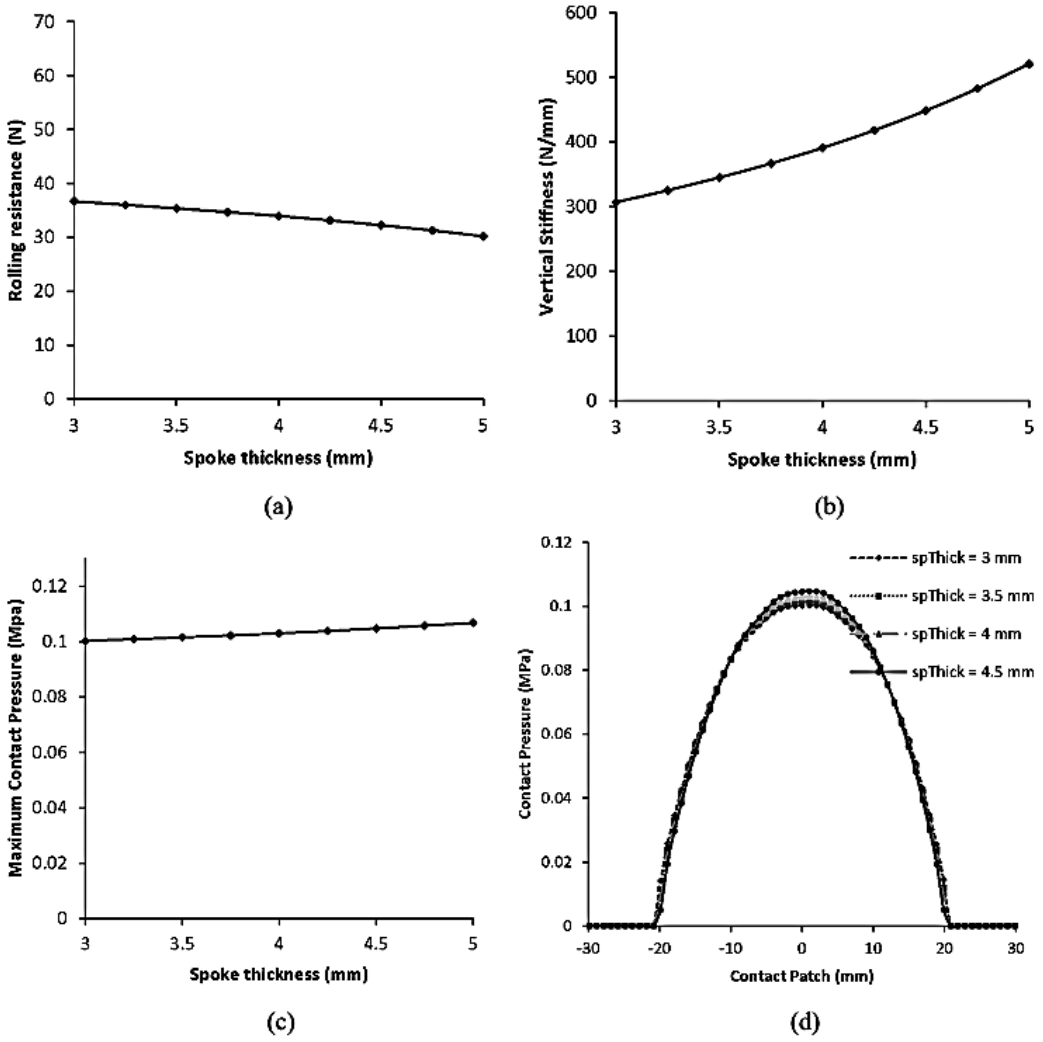

Figure 2.17: Effect of change in spoke thickness on NPT behavior

(Veeramurthy et al., 2014)

Jin et al. (2018) numerically simulated behaviors of NPTs with honeycomb spokes under static and dynamic conditions using commercial finite element analysis software ABAQUS. NPTs with honeycomb spokes having same load bearing capacity or the thickness of cell wall were considered. It was concluded that NPT with lowest cell angle had lowest mass of spokes, highest load bearing capacity and lowest rolling resistance (Figure 2.18).

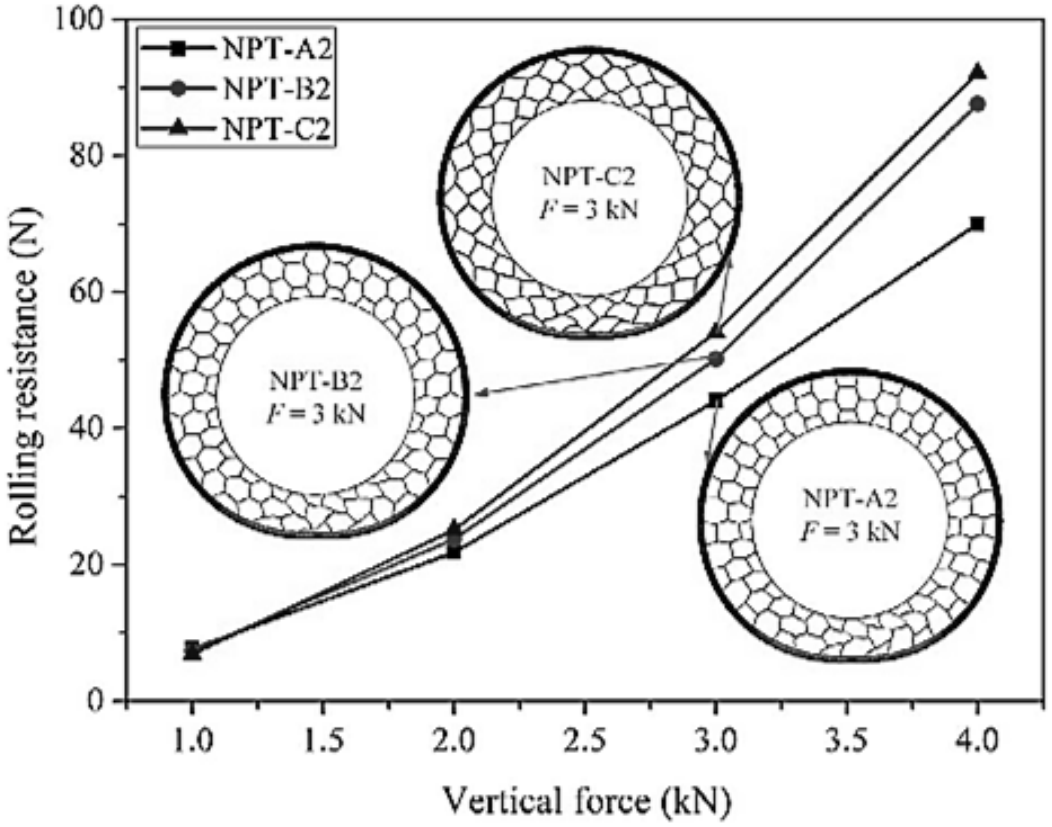

Figure 2.18: Rolling resistance under different vertical loads (A2 with lowest cell angle while C2 with highest cell angle)

(Jin et al., 2018)

Review shows that though literature is available on static and dynamic behaviors of NPTs yet there is less evidence of published literature on cornering characteristics of a NPT with hexagonal lattice spokes and their effect on handling and stability of a vehicle. Same is focused in this research.

CHAPTER 3: FINITE ELEMENT MODELLING AND MATERIAL PROPERTIES

3.1 Introduction

Finite element (FE) modeling plays an increasingly important part in investigation of static and dynamic behaviors of NPTs. Researchers and manufacturers emphasized correct modeling of tires to study through finite element modeling. Generation of an accurate three dimensional model is very important for further simulations under different working conditions. Basic requirements for generating the model include correct tire geometry and assigning precise tire material properties. A NPT with regular hexagonal spokes is selected for analysis with ABAQUS/Explicit. FE model of NPT is shown in Figure 3.1.

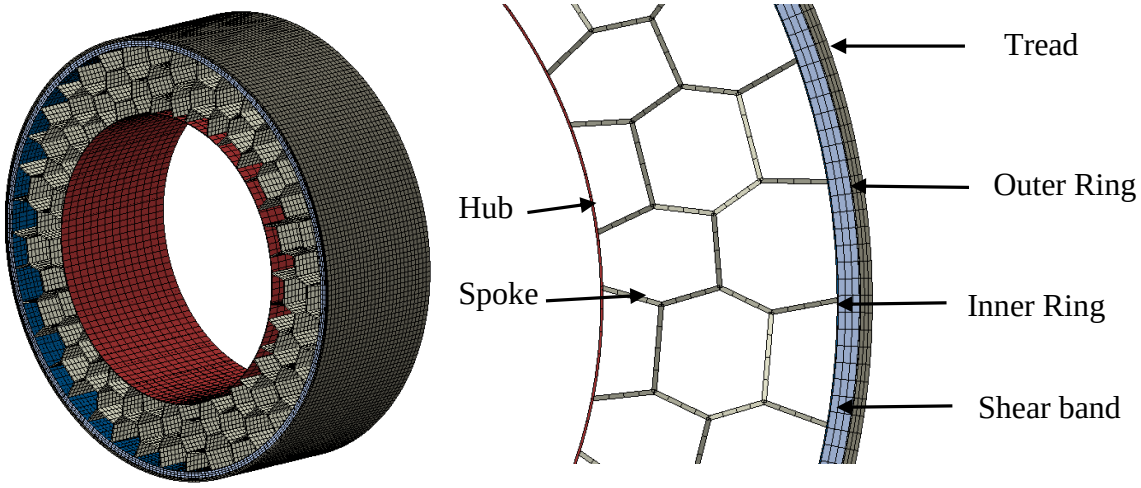

Figure 3.1: Finite element model of NPT with hexagonal lattice spokes

3.2 Components of a NPT with Hexagonal Lattice Spokes

NPT consists of the following components as shown in Figure 3.1:

a. Hub
b. Inner and outer rings
c. Flexible hexagonal lattice spokes
d. Shear band
e. Tread

Inner and outer rings sandwich the shear band in between them. NPT has inner radius of 216 mm and outer radius of 332 mm. Model has tire width of 215 mm. Remaining NPT

design parameters are tabulated in Table 3.1(Jin et al., 2018):

Table 3.1: Design Parameters of NPT Components

Component	**Hub**	**Lattice spokes**	**Inner and outer rings**	**Shear band**	**Tread**
Thickness(mm)	1	2	0.5	9	5

Design of the spokes structure includes number of parameters like cell height h, cell inclined length l and cell opening angle θ. Due to circular nature of structure of the NPT, these spokes cannot be designed with a single standardized h, l and θ. Design values of different parameters of spokes are shown in Figure 3.2 are given is Table 3.2.

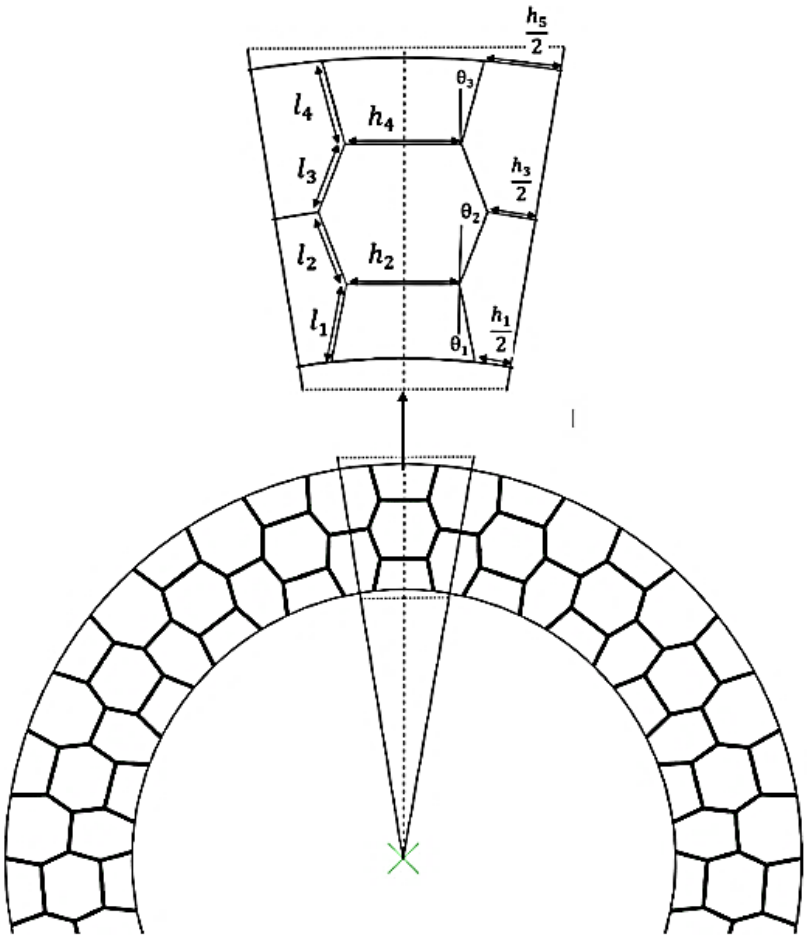

Figure 3.2: Design of hexagonal lattice spoke

It is clarified here that these values are arbitrarily chosen and may not necessarily represent the optimal values for cell design for cornering behavior of tire.

Table 3.2: Design Parameters of Hexagonal Lattice Spoke

Parameter	l_1	l_2	l_3	l_4	h_1	h_2	h_3	h_4	h_5	θ_1	θ_2	θ_3
Value mm/degree	26	26	24.44	28.56	24.12	37.62	31.91	38.73	50.92	11	21	15.28

3.3 Material Properties

PT consists of different parts that exhibit diverse material properties and behaviors. These include materials having linear elastic properties like metals and the materials having hyper –viscoelastic behavior like PU and rubber.

3.3.1 Linear Elastic Materials

Hub of the NPT is modelled as aluminum alloy (7075-T6) while inner and outer rings are modeled as high strength steel (ANSI-4340). Elastic properties of aluminum alloy and steel are given in Table 3.3(Jin et al., 2018).

Table 3.3: Properties of Metal Components

Material	**Young's Modulus (GPa)**	**Poisson's Ratio**	**Shear Modulus (GPa)**	**Density kg/m^3**
Aluminum alloy	72	0.33	27	2800
High Strength Steel	210	0.29	76	7800

3.3.2 Hyperelastic Materials

Shear band and hexagonal spokes are made of PU while tread is modelled with rubber. Hyper-viscoelastic model is used for both PU and rubber. Figures 3.3 and Figure 3.4 represent uniaxial, biaxial and planer test data of PU and rubber available in literature (J Ju et al., 2013). Appropriate constitutive relationship is required by fitting material behavior models for experimental stress-strain data.

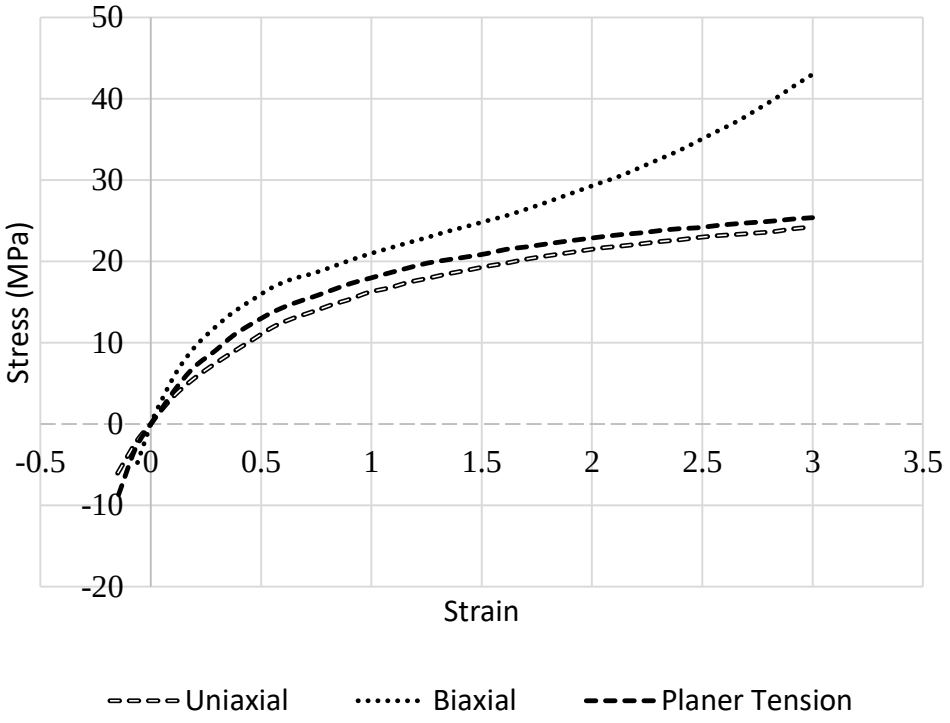

Figure 3.3: Non-linear stress strain behavior of PU

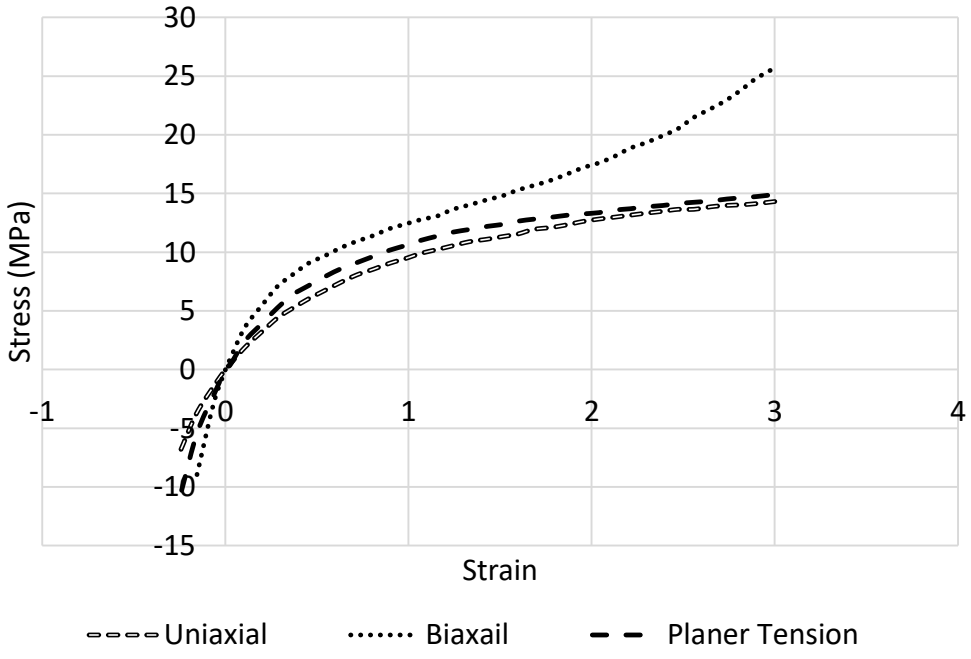

Figure 3.4: Non-linear stress strain behavior of rubber

Developers and researchers have used different hyperelastic models for rubbers and rubber like materials. Kim et al. (2012) compared hyperelastic models like Mooney rivlin, Neo-Hookean and Ogden models for chloroprene rubber. Ogden model was recommended for numerical analysis.

Marckmann and Verron (2006) thoroughly compared twenty different hyperelastic material models for rubber like materials (Table 3.4). These models were compared basing on validity range, number of material parameters and ability to reproduce different sets of experimental data with same set of material parameters. These models included both classical models and latest models which were not being used for industrial applications. Basing on the ranking first four models were separated which were able to fit all experimental data. Ogden model was among those four models which were widely used for numerical simulations. However, it required large experimental data for its six material parameters.

Table 3.4: Ranking of 20 Hyperelastic Models for Rubber-like Materials

Model	Year	Number of material parameters	Physics based
Extended Tube	1999	4	x
Shariff	2000	5	
Micro-Sphere	2004	5	x
Ogden	1972	6	
Haines-Wilson	1975	6	
Biderman	1958	4	
Hatr-Smith	1966	3	
8-chain	1993	2	x
Gent	1996	2	
Yeoh and Fleming	1997	4	
Van der Waals	1986	4	x
3-Chain	1943	2	x
Tube	1997	3	x
Mooney	1940	2	
Ishihara	1951	3	x
Gent and Thomas	1958	2	
Slip link	1981	3	x
Constrained Junctions	1982	3	x
Neo-Hookean	1943	1	x
Valanis and Landel	1967	1	

Rugsaj and Suvanjumrat (2018) investigated hyperelastic models to find out appropriate model for hyperelastic materials used in non-pneumatic tires. Experiments were performed on a specimen of PU obtained from Tweel. After obtaining experimental test data, test models were

validated. It was concluded that Mooney rivlin model showed good results in tensile tests while Ogden model better represented test data in compressive tests (Table 3.5).

Table 3.5: Averaged Error and Analysis Time of Hyperelastic Material Models Comparing to the Physical Experiment

Method	Percentage of average error (%)			Analysis time (sec)		
	Neo-Hookean	Mooney-Rivlin	Ogden	Neo-Hookean	Mooney-Rivlin	Ogden
Tensile test	61.90	17.07	19.30	3.53	143.83	151.85
Compressive test	53.32	24.07	5.61	125.11	5.58	5.01

Ali (2010) carried out review of different models for hyperelastic materials which are used in finite element analysis models. Strain energy density function of different models was fitted for experimental data by using softwares to minimize fitting error. It was concluded that selection of appropriate model depended on domain of deformation under consideration. For example, for general classification Neo-hooken model could be used for small strains while Mooney and Ogden models could be used for moderate and large strain applications. Basing on the review of literature on hyperelastic modeling and material models used by researchers in modeling of NPT, hyperelastic behavior of polyurethane and synthetic rubber is modelled by Ogden hyperelastic model. Strain energy function of Ogden hyperelastic model with N=3 is given by equation 3.1 (Ogden, 1972).

$$W(\lambda_1, \lambda_2, \lambda_3) = \sum_{i=1}^{N} \frac{\mu_i}{\alpha_i} (\lambda_1{}^{\alpha_i} + \lambda_2{}^{\alpha_i} + \lambda_3{}^{\alpha_i} - 3) \quad (3.1)$$

Here λ_i represent stretches in principal direction, μ_i and α_i are temperature dependent material parameters, while N is a material parameter.

3.3.3 **Viscoelastic Material Properties**

Viscoelastic behavior of PU is implemented with time dependent viscoelastic model using Prony series based on shear relaxation. Prony series is given by Equation 3.2(DS Simulia, 2009; Jin et al., 2018).

$$G_R(t) = G_0 \left[1 - \sum_{i=1}^{N} g_i (1 - e^{-t/\tau_i}\right] \quad (3.2)$$

here $G_R(t)$ and G_0 are shear relaxation and instantaneous shear moduli of the material. g_i and τ_i represent i^{th} Prony constant and Prony relaxation time constant while t is the time. Constants of equation 3.2 for PU and rubber are given in Table 3.6(Jin et al., 2018).

Table 3.6: Viscoelastic Properties of PU and Rubber

	Polyurethane		**Rubber**	
i	g_i	τ_i	g_i	τ_i
1	0.125	0.002	0.200	0.002
2	0.125	0.020	0.200	0.020
3	0.125	0.200	0.200	0.200

3.4 Meshing and Element Properties

Hub, hexagonal lattice spokes and rings are modelled using shell element (S4R). Mesh density is kept almost double for the hyperelastic components which undergo large deformations during loading and rolling. Due to lesser thickness, spokes are modelled with 4 node S4R shell elements. Shear band & tread are modelled using solid 8 node brick element C3D8R. Three elements are used along the thickness of tread and shear band to cater for shear effects. Tread and shear band have same number of elements along width and circumference. Number of elements along circumference are about ten times more than the width. Hub and rings have half the number of elements along width and circumference as compared to tread. Mesh density of spokes is kept similar to tread along tire width.

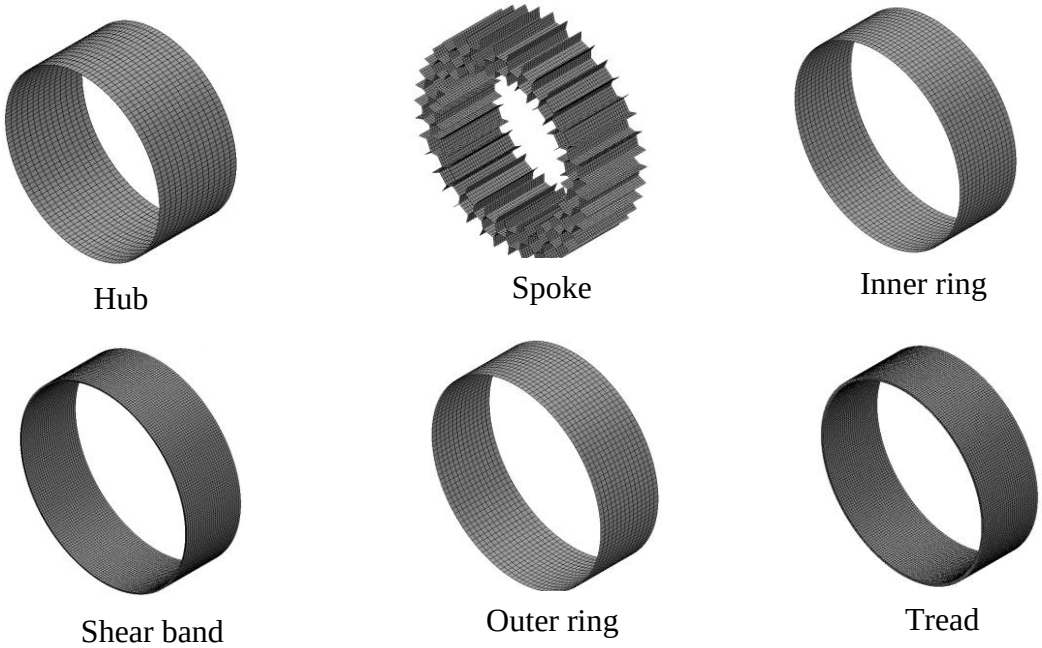

Figure 3.5: Finite element mesh

3.5 Constraint and Interactions

A reference point (RIM) is created at center of NPT to act as control point. Rigid kinematic interaction is defined between reference point and hub through kinematic coupling in ABAQUS. Tie constraint is used to assemble tread, shear band, rings, spokes and hub. Road is modelled as analytical rigid surface. Thus there is no deformation of ground under loading. Simulation wholly represents the behavior of tire in contact with road. Displacement of road is controlled as rigid body through a reference point (ROAD) located right under RIM at road surface. Interaction of road and tire is defined by surface-to-surface contact. Contact friction is modelled in tangential direction while hard contact is assumed in normal direction. Coefficient of friction (μ) is kept as 0.15 in static simulations. In order to keep rolling conditions at par with the PT data to be compared with NPT, coefficient of friction 1 is used during NPT dynamic simulations.

3.6 Loads and Boundary Conditions

Research objective is to investigate cornering characteristics of NPT. However, static loading of tire is also executed to benchmark the FE model with published data. Thus analysis comprises of two separate procedures.

3.6.1 Static Loading

First procedure consisting of static general analysis is performed to find the behavior of NPT under static loading conditions.

3.6.1.1 Loads

NPT is subjected to a vertical load at reference point. The load is ramped up to 4000 N in different steps with increments of 1000 N.

3.6.1.2 Boundary Conditions

Two different boundary conditions are defined. Initially, all degrees of freedom of RIM are constrained and ROAD is also constrained is all DOF except in Z direction. ROAD is then made to contact with tire outer surface through boundary condition in Z direction after which it is constrained there in all DOF. Once contact is made then RIM is made free only in Z degree of freedom for application of load in that direction. Vertical deflection of NPT is measured by vertical movement of RIM, from field output data.

3.6.2 **Cornering**

Once the model is benchmarked then cornering is simulated in second procedure with explicit procedure. Cornering procedure itself consists of two parts, in which, first part is loading of tire at reference load while the second part is rolling of tire under cornering conditions (Figure 3.6).

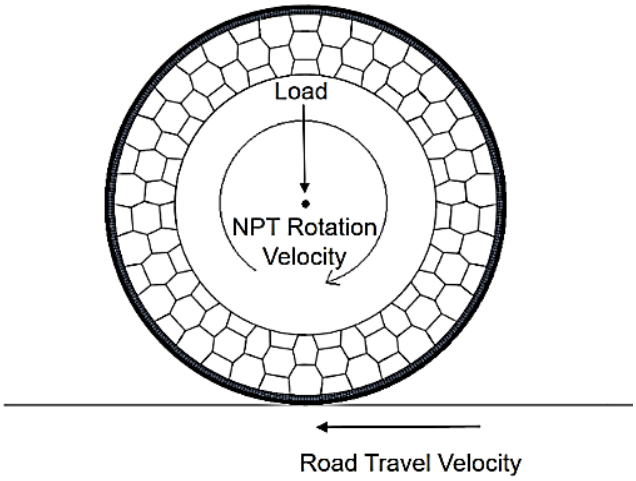

Figure 3.6: Loading and rolling description

3.6.2.1 **Loads**

NPT is loaded with vertical loads of 1594N, 2000N and 2500N in different simulations as per aim of the procedure. Load is maintained during second part of procedure.

3.6.2.2 **Boundary Conditions**

Similar to static loading, two boundary conditions are defined. Contact is established and load is applied as per the process followed in static loading. Once loading is done, then in addition to Z direction, RIM is also set free to rotate around its center, while remaining DOF are kept constrained. Cornering conditions are then applied on ROAD by application of velocity boundary conditions in its plane through velocities V_x and V_y in X and Y directions. These velocities are calculated against the desired slip angles as already discussed.

CHAPTER 4: RESULTS AND DISCUSSION

Results of the research can be distributed into two parts. In first part, results of finite element analysis carried out using ABAQUS are described, while in second part findings of vehicle dynamics from CARSIM are discussed.

4.1 Finite Element Analysis(FEA)

Static loading and steady state cornering analysis of NPT has been carried out using FEA.

4.1.1 Static Analysis

Modelled NPT is statically loaded to find out static deflection under different vertical loads. Deflections are measured from center reference point of tire. Results are plotted as shown in Figure 4.1.

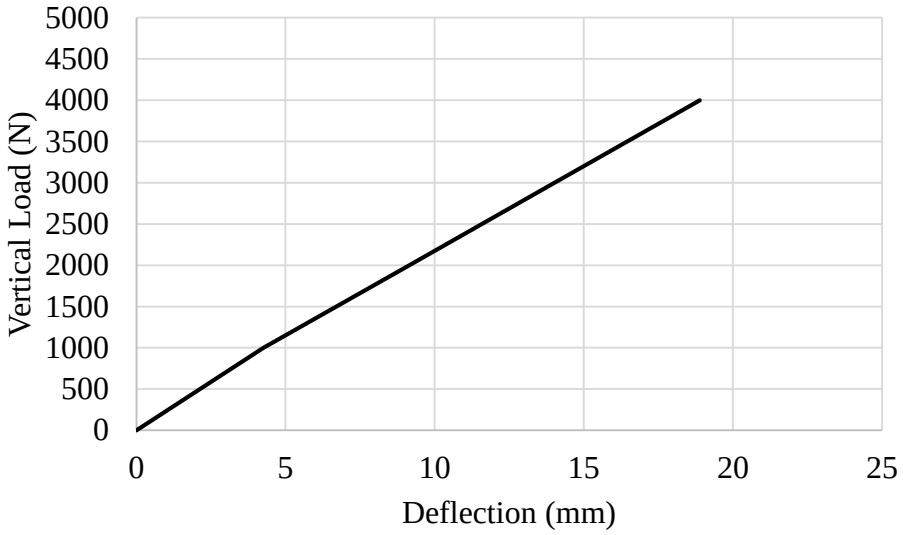

Figure 4.1: Static loading

According to mesh convergence study(Jin et al., 2018) 40 elements (approximate average element size of 5.2mm) along the width of tire for tread are selected for the further simulations. Mesh size of remaining parts is adjusted accordingly as discussed in Chapter 3. Results of static loading are compared with published data of NPT (Jin et al., 2018) as shown in Figure 4.2. Comparison shows closer results with a maximum error of about 13%. Since the curve fitting for hyperelastic model and resultantly calculated material parameters affects the behavior of hyperelastic materials therefore this error seems to be caused by difference of curve fitting methods used to calculate material parameters. Basing on these results the developed finite element model of the NPT stands

benchmarked to be used for further simulations.

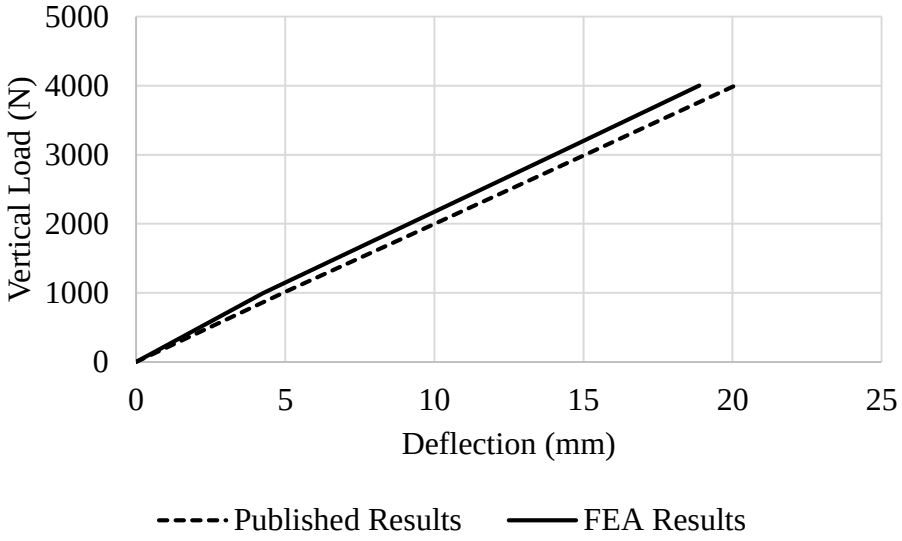

Figure 4.2: Comparison of NPT and PT under static loading

4.1.2 **Steady State Cornering Analysis**

Objective of steady state cornering simulation is to determine lateral forces and aligning moments generated at different slip angles. A steady state cornering is the state at which there is no breaking or accelerating force acting on the NPT. Thus it is a state of negotiating a turn that is having a slip angle while fulfilling the conditions of free rolling. Cornering is achieved through the modeling arrangements explained in earlier sections. In order to find forces and moments at steady state condition, tire is allowed to make minimum 1.5 rotations so that it reaches free rolling condition at a given slip angle before calculating the values. Initially cornering is performed at vertical load of 1594 N at different slip angles with increment of 0.5^o ranging from 0^o to 2.5^o of slip angle. Extensive research has been carried out by the researchers on cornering behavior of pneumatic tires, therefore it is felt necessary to study cornering behavior of NPT with that of a PT of similar size.

4.1.2.1 **Cornering Force**

Time history of simulations at different slip angles under vertical load of 1594 N is shown in Figure 4.3 and 4.4. Time history shows that at lower slip angles, steady state cornering condition is achieved earlier. PT has some value of lateral force even at zero slip angles (Figure 2.6) due to ply steer, however since NPT don’t have any such component therefor about zero lateral force is observed at zero slip angle.

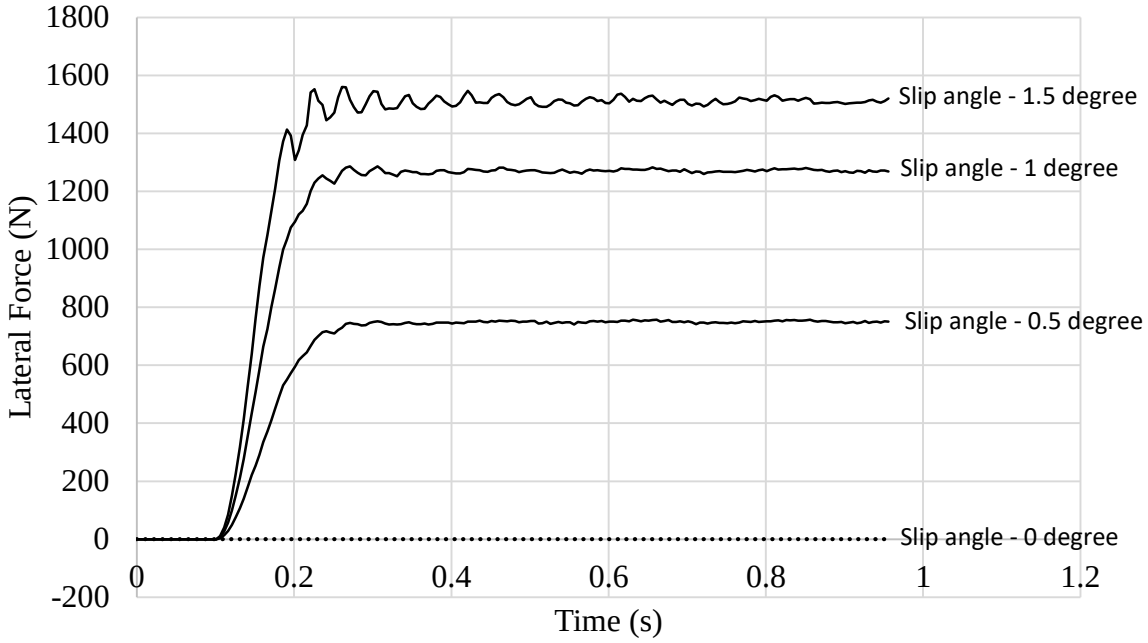

Figure 4.3: Time history of cornering force at vertical load of 1594 N, at lower slip angles

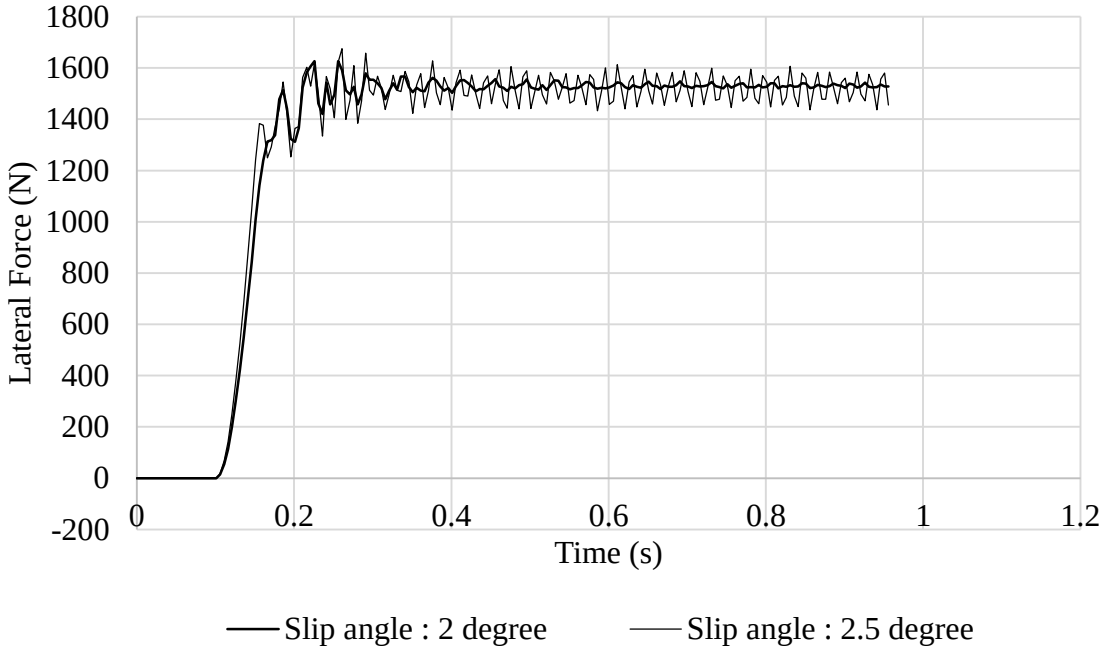

Figure 4.4: Time history of lateral force at vertical load of 1594 N, at higher slip angles

Average values of the lateral force under steady state cornering condition is plotted in Figure 4.5. Results are also compared with a PT of similar size under same loading conditions. Lateral force increases with slip angle till it reaches a maximum value closer to

μ times the vertical load applied. At lower slip angles tire elastic properties play major role, while at higher slip angles, where behavior of lateral force and slip angle curve is non-linear, tire road traction properties become dominant. Comparison of NPT and PT clearly show that cornering stiffness of NPT is higher than the PT. Higher cornering stiffness is due to greater out of plane (lateral) stiffness of hexagonal lattice spokes of NPT. Peak value of lateral force for NPT is also achieved at lesser slip angles due to this phenomenon.

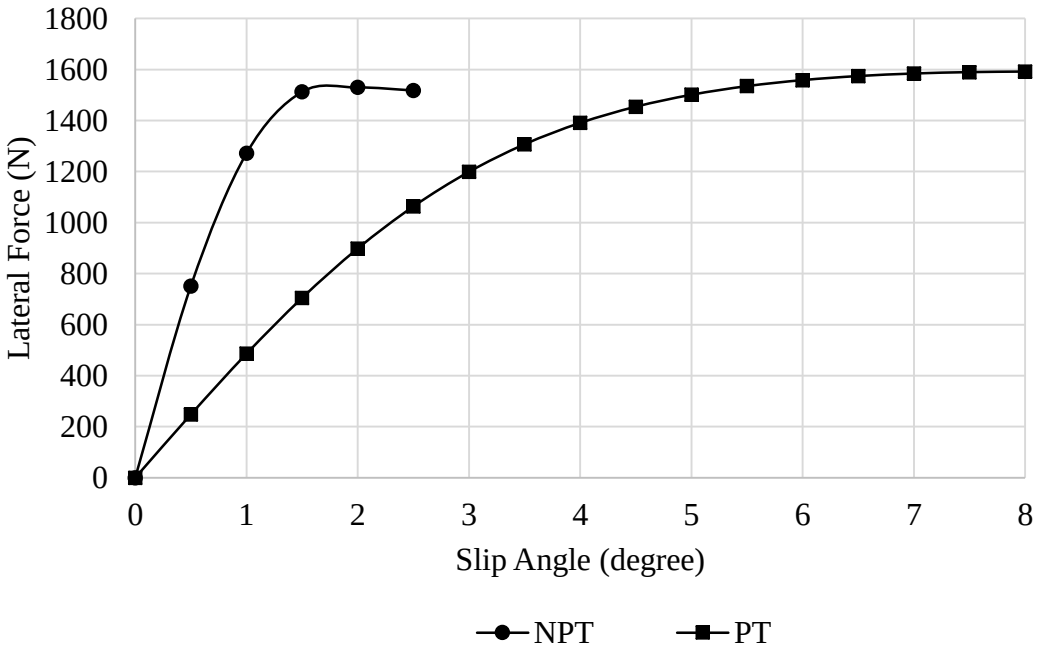

Figure 4.5: Comparison of lateral forces at 1594 N

It is well known that cornering stiffness of PTs increase with increase in vertical load. NPT vertical load is also increased and simulation results are obtained for vertical loads of 2000N and 2500N (Figure 4.6). Cornering stiffness of NPT increases with vertical load similar to PT. Another observation shows that though saturation of lateral force is achieved at lower slip angle for NPT, overall shape of the lateral force verses slip angle plot of NPT is similar to a typical PT.

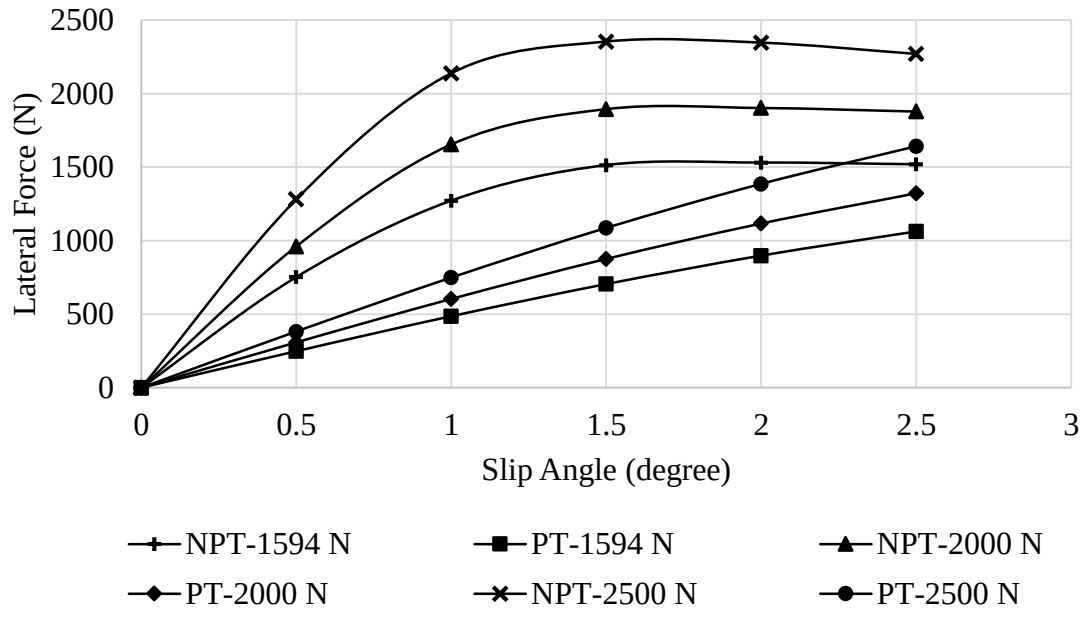

Figure 4.6: Comparison of lateral forces at different loads and slip angles

Time history of cornering force under different loads is plotted in Figure 4.7. Plots show that time to reach steady state cornering condition is not much affected by the increase in vertical loads at same slip angles.

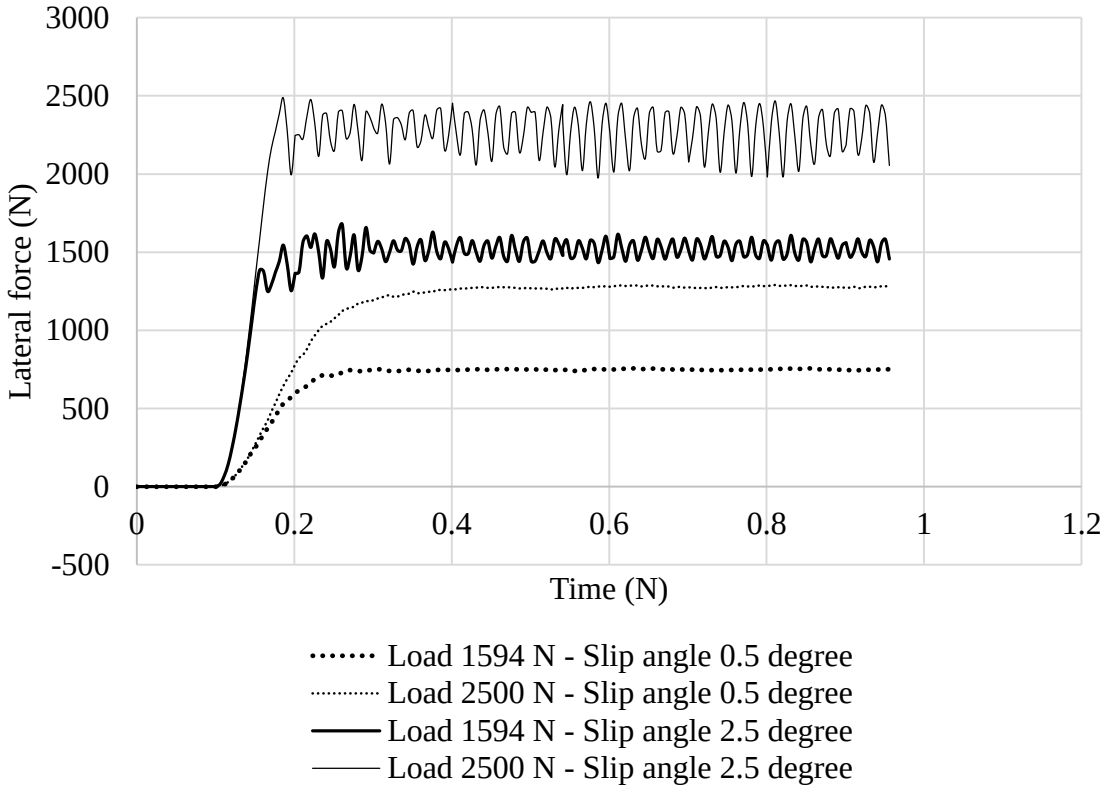

Figure 4.7: Time history of lateral force at different loads and slip angles

4.1.2.2 **Aligning Moment**

Average values of steady state aligning moment produced at various slip angles during simulations are calculated and compared with the pneumatic tire as shown in Figure 4.8. Assessment shows that aligning moments has much lesser value of peak aligning moment which is achieved at a lower slip angle than the pneumatic tire. As the lateral force starts to build with cornering, pneumatic trail increase causing increase in value of aligning moment. Resultant lateral force moves away from origin till aligning moment approaches its peak value. Further increase in lateral force cause decrease in pneumatic trail, resultantly aligning moments starts to decease. At large slip angles, resultant force may even move ahead of the origin causing change in sign of the aligning moment. It is obvious from Figure 4.8 that direction of aligning moment also changes earlier in case of NPT. Reason of this behavior lies in early peak value of lateral force which effects aligning moment to reach maximum value at lower slip angles. Tire deformation is lesser in NPT due to greater cornering stiffness, therefore peak value of aligning moment is also lower.

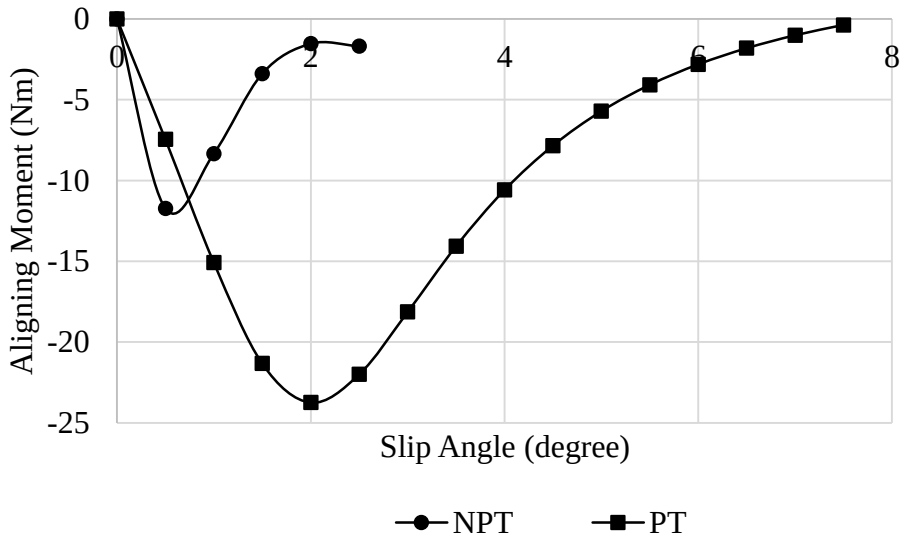

Figure 4.8: Comparison of aligning moment at 1594 N

Behavior of aligning moment with increase in vertical load is presented in Figure 4.9. Peak value of aligning moment also increases with increase in vertical load, however there is a clear difference in peak values of aligning moment for PT and NPT.

Behavior of lateral force and aligning moment of NPT under different loading conditions and at various slip angles in comparison with PT show that though there is difference in

peak values yet overall behavior of plots for NPT is similar to the PT (Figure 2.6).

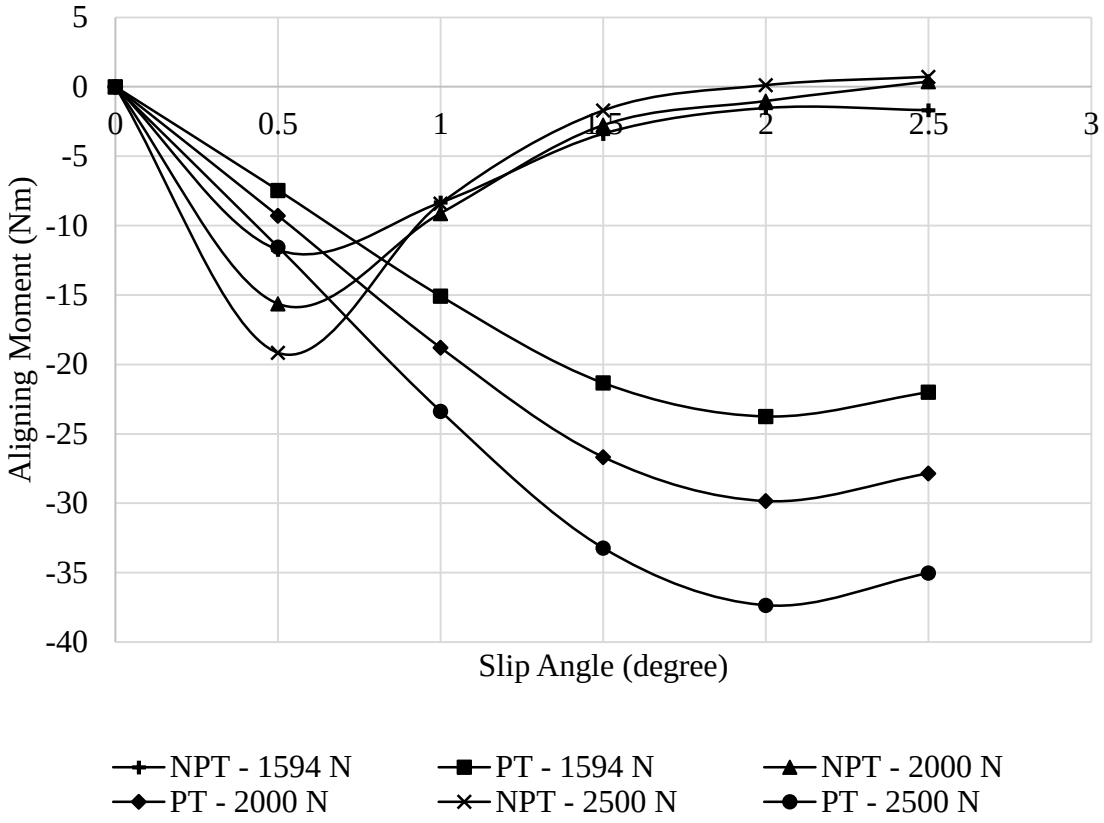

Figure 4.9: Comparison of aligning moment at different loads and slip angles

4.2 Vehicle Dynamic Analysis

Cornering stiffness is one of the most important factors that affect handling and directional stability of a vehicle. In previous section it has been found through FEA results that NPT cornering stiffness is much higher than the pneumatic tire. In order to find effect of this behavior on overall vehicle performance, a professional vehicle dynamics software, CARSIM, has been used. CARSIM have different inbuilt tire models. Input for these tire models is provided in the form of parameters of those models. CARSIM also provides opportunity to provide input of tire dynamic behaviour through tire properties tables. CARSIM inbuilt model then uses this data to simulate dynamic behaviour of tire. NPT data obtained through FEA is fed into CARSIM through this opportunity. Default data and build-in testing module was used for PT of similar size. Dynamic behaviour of vehicle with both tires is compared through limiting test procedures designed for handling and stability of a vehicle. These procedures include double lane change and fixed time fishhook procedures. Details of these procedures is described in detail in earlier sections. Same vehicle is used for dynamic analysis using NPT and PT during double lane change and fishhook

procedures. Exclusive input of PT and NPT data will assist in study of changes in vehicle dynamics due to change in tires. Keeping in view the aim of simulations, more emphasis is given on analysis and interpretation of steering handwheel angle, lateral acceleration, yaw rate of sprung masses, and roll angle of vehicle.

4.2.1 **Double Lane Change (DLC)**

DLC manoeuvre was performed separately with NPT and PT. Figure 4.10 show inputs given through steering handwheel to complete the manoeuvre. It is visible from the plot that the vehicle with NPT requires lesser input of steering handwheel. Lesser input indicates that vehicle responded more with lesser rotation of steering. Thus response of the vehicle is increased with addition of NPT.

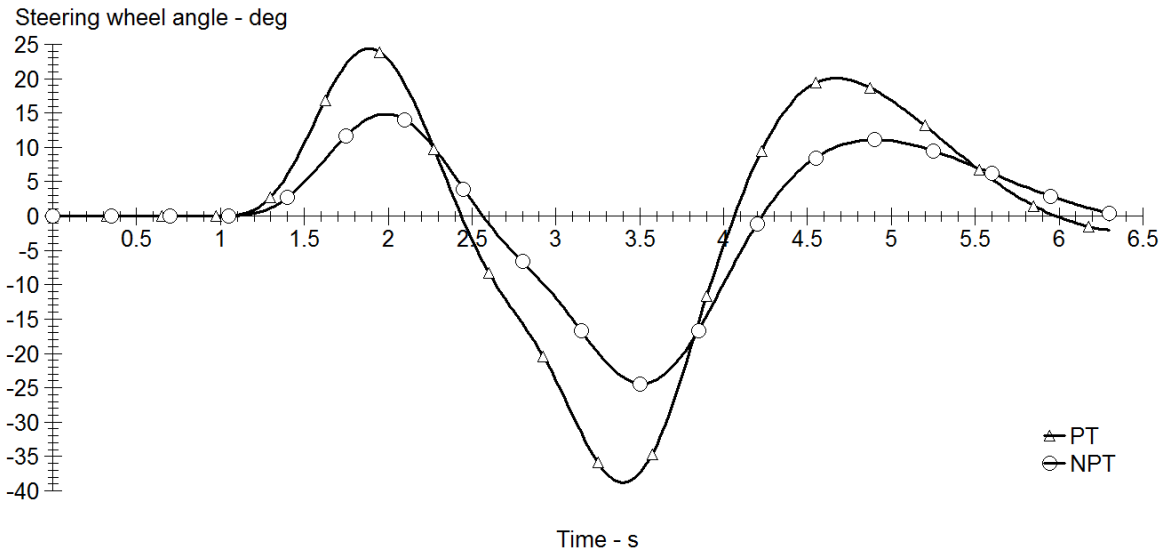

Figure 4.10: Comparison of NPT and PT – Steering wheel angle (DLC)

Figure 4.11 is plot of yaw rate of sprung masses. Yaw rate is measure of vehicle handling. Decrease in yaw rate makes handling and control easier for the driver. Here a visible decrease in yaw rate of vehicle is observed with NPT which indicates improvement in handling and control.

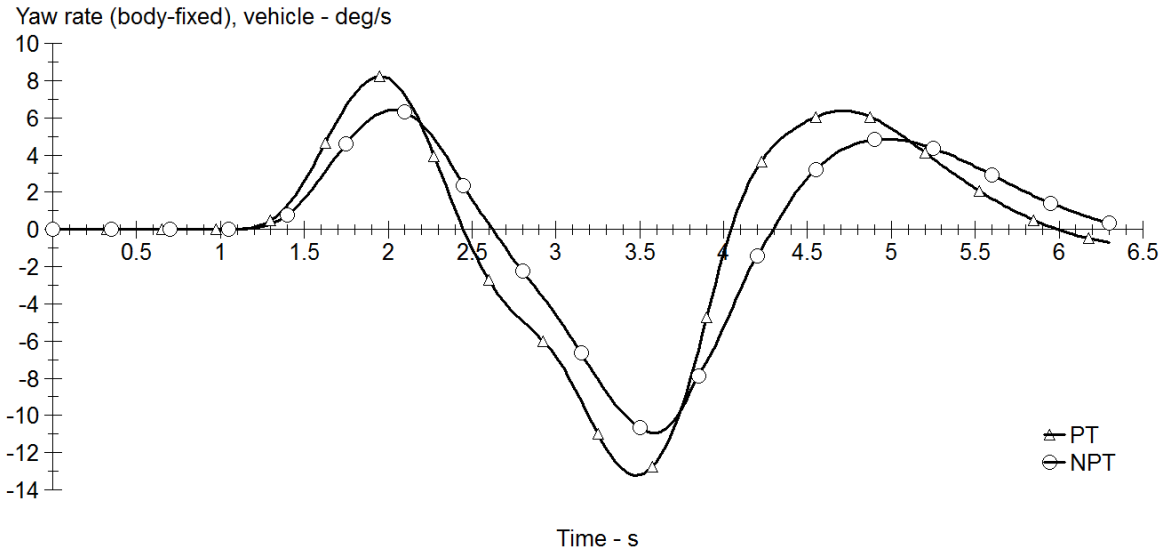

Figure 4.11: Comparison of NPT and PT – Yaw rate (DLC)

Ground vehicle dynamic stability is a complex matter which involves many factors. Roll angle and lateral acceleration are among the important factors that affect stability of a vehicle. In Figures 4.12 and 4.13, lateral acceleration and roll angle for PT and NPT fitted vehicles are compared. There is no considerable difference between the behaviour. The reason is that DLC is not a limiting manoeuvre for roll stability of the vehicle so here no clear increase or decrease in vehicle stability performance is observed.

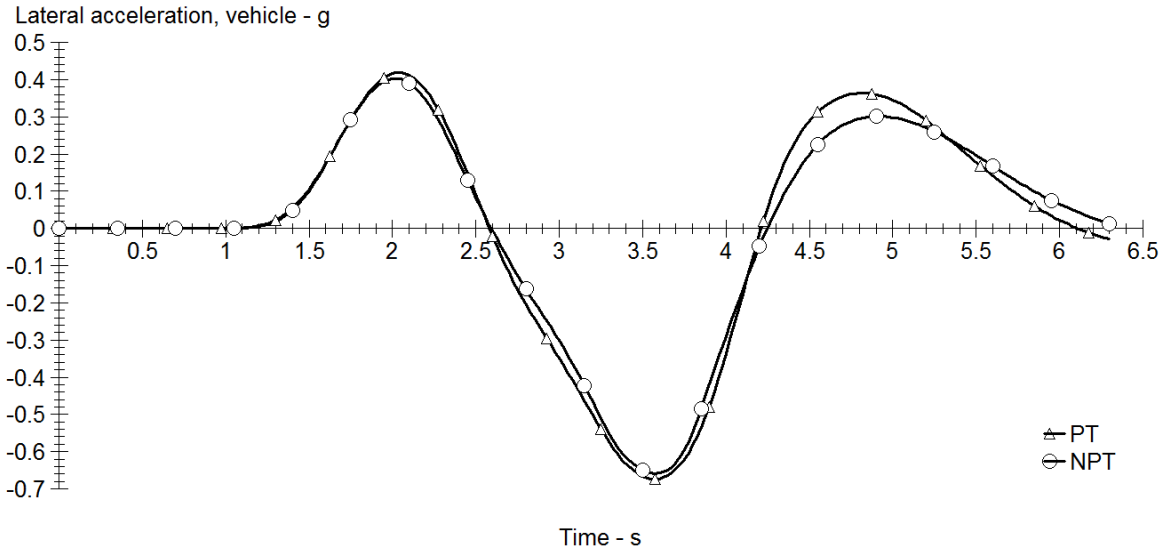

Figure 4.12: Comparison of NPT and PT – Lateral acceleration (DLC)

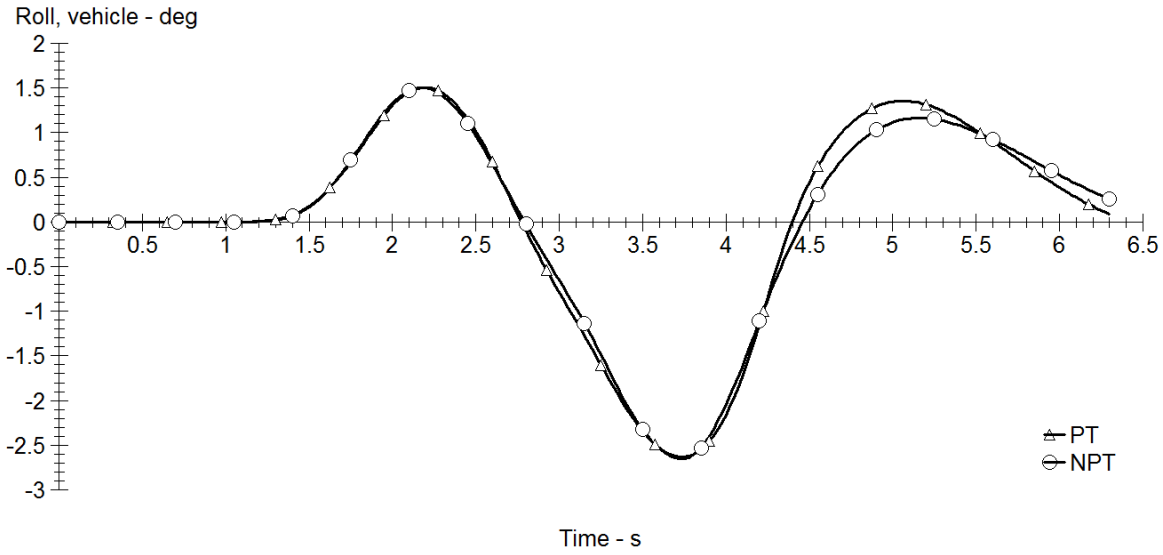

Figure 4.13: Comparison of NPT and PT – Roll angle (DLC)

4.2.2 **Fishhook (FH)**

Fixed timing fishhook procedure is performed in two steps. In first step the SIS angle for vehicles with NPT and PT is found at 80 Km/h. Then fishhook maneouvre is performed as already discussed in section 2.8.2. CARSIM caters for all design parameters required for completion of the procedure. Figure 4.14 shows input of steering handwheel during the maneuver. Steering input difference between fishhook maneuver for NPT and PT is due to higher longitudinal stiffness of NPT which requires lesser steering input to reach 0.3g lateral acceleration in SIS. Longitudinal dynamics of the vehicle and tire are not focus of interest in this research therefore these are not discussed here. It is visible from comparison that the response of vehicle during fishhook maneuver is increased in case of NPT. Figure 4.15 displays yaw rate of sprung masses during fishhook maneuver, here again a considerable decrease in yaw rate of sprung masses is observed.

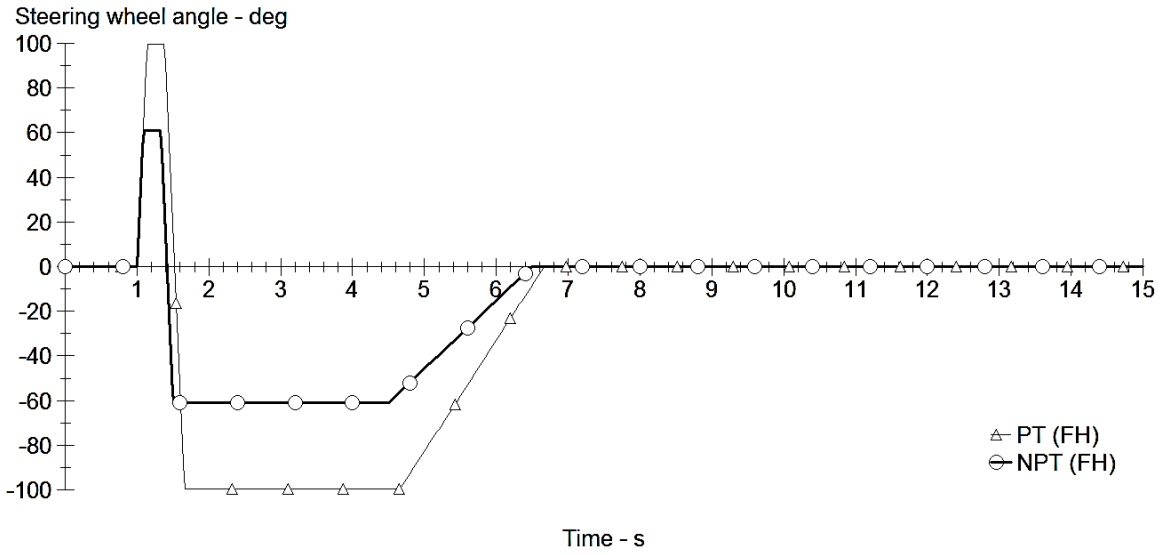

Figure 4.14: Comparison of NPT and PT – Steering wheel angle (FH)

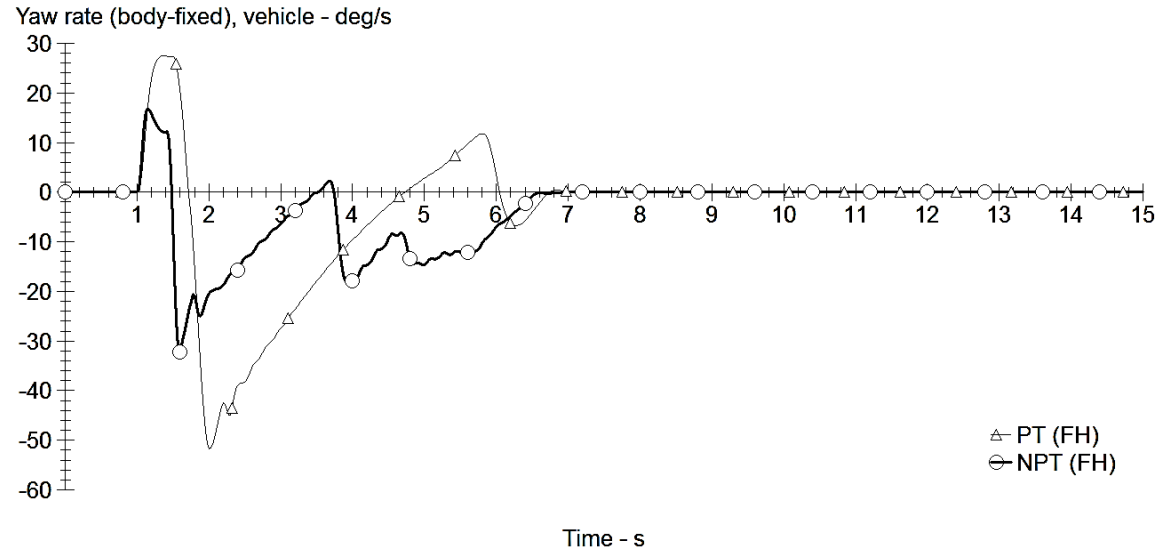

Figure 4.15: Comparison of NPT and PT – Yaw rate (FH)

Figure 4.16 displays comparison of tires for lateral acceleration. Here we don't find any comparable difference, however Figure 4.17 and 4.18 illustrate increase in vehicle roll angle and roll rate due to NPT.

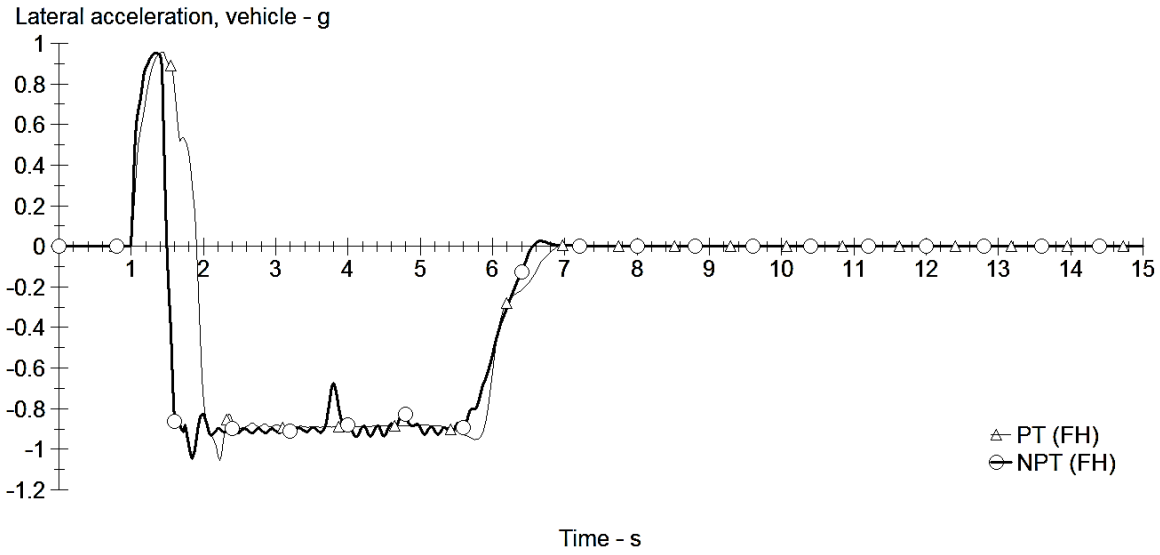

Figure 4.16: Comparison of NPT and PT – Lateral acceleration (FH)

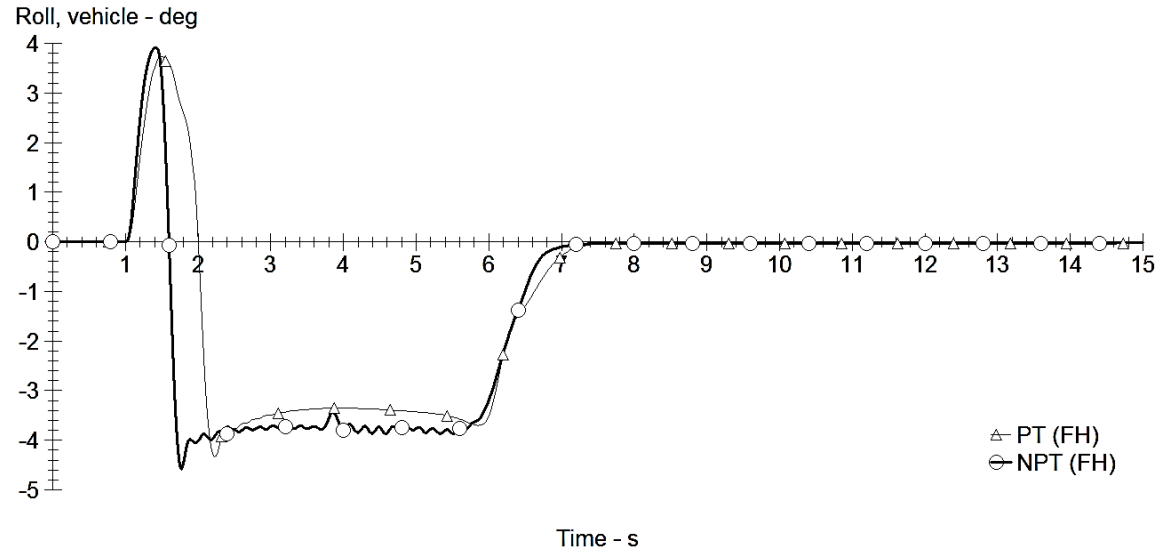

Figure 4.17: Comparison of NPT and PT – Roll angle (FH)

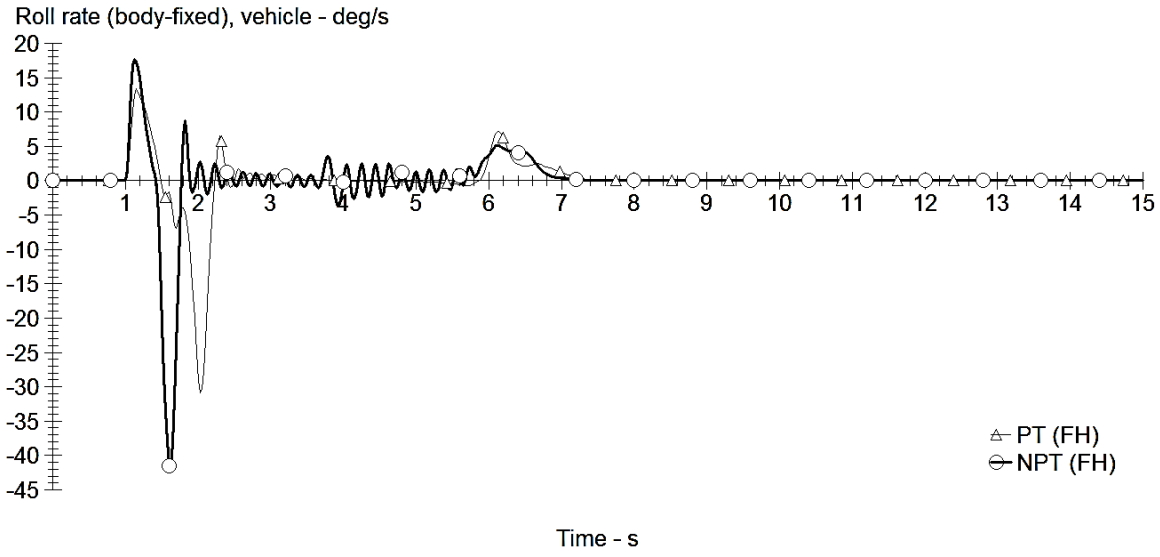

Figure 4.18 : Comparison of NPT and PT – Roll rate (FH)

Higher roll rate enhances roll over propensity of vehicle by shifting the load to outer wheels due to momentum. Vehicle having high center of gravity are more effected by shift of center of gravity. Thus such vehicle, fitted with NPTs, running at high speeds by an inexperienced driver is more prone to roll over.

CHAPTER 5: CONCLUSIONS

In this study, cornering characteristics of a non-pneumatic tire with hexagonal lattice spokes are investigated using finite element analysis code ABAQUS and compared with a pneumatic tire of similar size. Effect of non-pneumatic tire cornering characteristics on handling and stability of a vehicle are also studied in CARSIM by double lane change and fishhook manoeuvres. Findings of the study are as under:

The studied “non-pneumatic tire with hexagonal lattice spokes” has higher cornering stiffness than pneumatic tire due to more out of plane stiffness of hexagonal lattice. Cornering stiffness and peak aligning moment of non-pneumatic tire increase with increase in vertical load.

Aligning moment of non-pneumatic tire has lesser peak value as compared to pneumatic tire which shows less steering effort. For same speed and vertical load, steady state cornering condition of non-pneumatic tire is achieved earlier with decrease in slip angle.

Higher cornering stiffness of non-pneumatic tire prominently enhances vehicle response and handling. However, greater roll rate in fishhook manoeuvre indicate increase in vehicle roll over propensity due to non-pneumatic tires in limiting manoeuvres at higher speeds.

Non-pneumatic tires have great potential to be used in military vehicles by improving their handling and availability. It may also prove life saver during military operations. However, greater response and high roll rate of non-pneumatic tire fitted vehicle require consideration at high speeds.

REFERENCES

Abe, M. (2015). Vehicle Handling Dynamics: Theory and Application: Second Edition. In *Vehicle Handling Dynamics: Theory and Application: Second Edition*. https://doi.org/10.1016/C2014-0-04001-4

Aboul-Yazid, A. M., Emam, M. A. A., Shaaban, S., & El-Nashar, M. A. (2015). Effect of spokes structures on characteristics performance of non-pneumatic tires. *International Journal of Automotive and Mechanical Engineering*, *11*(1), 2212–2223. https://doi.org/10.15282/ijame.11.2015.4.0185

Ali. (2010). A Review of Constitutive Models for Rubber-Like Materials. *American Journal of Engineering and Applied Sciences*, *3*(1), 232–239. https://doi.org/10.3844/ajeassp.2010.232.239

Allen, R. W., Myers, T. T., Rosenthal, T. J., & Klyde, D. H. (2000). The effect of tire characteristics on vehicle handling and stability. *SAE Technical Papers*. https://doi.org/10.4271/2000-01-0698

Balawi, S., & Abot, J. L. (2008). The effect of honeycomb relative density on its effective in-plane elastic moduli: An experimental study. *Composite Structures*, *84*(4), 293–299. https://doi.org/10.1016/j.compstruct.2007.08.009

Cao, J., Jing, L., Guo, K., Engineering, F. Y.-M. P. in, & 2013, U. (2013). Study on integrated control of vehicle yaw and rollover stability using nonlinear prediction model. *Hindawi.Com*. Retrieved from https://www.hindawi.com/journals/mpe/2013/643548/abs/

Celeri, F., & Chiesa, A. (1974). A Method for the Evaluation of the Lateral Stability of Vehicles and Tires. *SAE Technical Paper 741101*. Retrieved from https://www.sae.org/gsdownload/?prodCd=741101

Chae, S. (2006). *Non linear finite element modeling and analysis of a truck tire*. Pennsylvania State University.

Deng, Y., Zhao, Y., Lin, F., Xiao, Z., Zhu, M., & Li, H. (2018). Simulation of steady-state rolling non-pneumatic mechanical elastic wheel using finite element method. *Simulation Modelling Practice and Theory*, *85*, 60–79.

https://doi.org/10.1016/j.simpat.2018.04.001

DS Simulia. (2009). *Abaqus 6.14*. Dessault.

Forkenbrock, G. J., Garrott, W. R., Heitz, M., & O'Harra, B. C. (2003a). An experimental examination of double lane change maneuvers that may induce on-road, untripped, light vehicle rollover. *SAE Technical Papers*. https://doi.org/10.4271/2003-01-1009

Forkenbrock, G. J., Garrott, W. R., Heitz, M., & O'Harra, B. C. (2003b). An experimental examination of j-turn and fishhook maneuvers that may induce on-road, untripped, light vehicle rollover. *SAE Technical Papers*. https://doi.org/10.4271/2003-01-1008

Gibson, L. J., Ashby, M. F., Schajer, G. S., & Robertson, C. I. (1982). MECHANICS OF TWO-DIMENSIONAL CELLULAR MATERIALS. *Proceedings of The Royal Society of London, Series A: Mathematical and Physical Sciences, 382*(1782), 25–42. https://doi.org/10.1098/rspa.1982.0087

Gillespie, T. D. (1992). Fundamentals of Vehicle Dynamics. In *Fundamentals of Vehicle Dynamics*. https://doi.org/10.4271/r-114

ISO. (2018). ISO 3888-1:2018(en), Passenger cars — Test track for a severe lane-change manoeuvre — Part 1: Double lane-change. Retrieved November 24, 2019, from https://www.iso.org/obp/ui/#iso:std:iso:3888:-1:ed-2:v1:en

Jin, X., Hou, C., Fan, X., Sun, Y., Lv, J., & Lu, C. (2018). Investigation on the static and dynamic behaviors of non-pneumatic tires with honeycomb spokes. *Composite Structures, 187*, 27–35. https://doi.org/10.1016/j.compstruct.2017.12.044

Ju, J, Veeramurthy, M., … J. S.-T. S. and, & 2013, U. (2013). Rolling resistance of a nonpneumatic tire having a porous elastomer composite shear band. *Tiresciencetechnology.Org*. Retrieved from https://www.tiresciencetechnology.org/doi/abs/10.2346/tire.13.410303

Ju, Jaehyung, Kim, D. M., & Kim, K. (2012). Flexible cellular solid spokes of a non-pneumatic tire. *Composite Structures*, *94*(8), 2285–2295. https://doi.org/10.1016/j.compstruct.2011.12.022

Kabe, K., & Koishi, M. (2000). Tire cornering simulation using finite element analysis. *Journal of Applied Polymer Science*, *78*(8), 1566–1572.

https://doi.org/10.1002/1097-4628(20001121)78:8<1566::AID-APP140>3.0.CO;2-I

Kim, B., Lee, S. B., Lee, J., Cho, S., Park, H., Yeom, S., & Park, S. H. (2012). A comparison among Neo-Hookean model, Mooney-Rivlin model, and Ogden model for Chloroprene rubber. *International Journal of Precision Engineering and Manufacturing*, *13*(5), 759–764. https://doi.org/10.1007/s12541-012-0099-y

Kim, K., Heo, H., Uddin, M. S., Ju, J., & Kim, D. M. (2015). Optimization of Nonpneumatic Tire with Hexagonal Lattice Spokes for Reducing Rolling Resistance. *SAE Technical Papers*, *2015-April*(April). https://doi.org/10.4271/2015-01-1515

Kim, K., & Kim, D. M. (2011). Contact pressure of non-pneumatic tires with hexagonal lattice spokes. *SAE 2011 World Congress and Exhibition*. https://doi.org/10.4271/2011-01-0099

Kim, K., Kim, D. M., & Ju, J. (2013). Static Contact Behaviors of a Non-Pneumatic Tire with Hexagonal Lattice Spokes. *SAE International Journal of Passenger Cars - Mechanical Systems*, *6*(3), 1518–1527. https://doi.org/10.4271/2013-01-9117

Koishi, M., Kabe, K., & Shiratori, M. (1998). Tire Cornering Simulation Using an Explicit Finite Element Analysis Code. *Tire Science and Technology*, *26*(2), 109–119. https://doi.org/10.2346/1.2135960

Marckmann, G., & Verron, E. (2006). Comparison of hyperelastic models for rubber-like materials. *Rubber Chemistry and Technology*, *79*(5), 835–858. https://doi.org/10.5254/1.3547969

Michelin. (2012). Welcome to Michelin Tweel Technologies News. Retrieved January 24, 2020, from https://michelintweel.com/tweelNews_10-29-12.html

NHTSA. (2013). *Laboratory Test Procedure for Dynamic Rollover The Fishhook Maneuver Test Procedure*.

Ogden, R. W. (1972). Large Deformation Isotropic Elasticity: On the Correlation of Theory and Experiment for Compressible Rubberlike Solids. *Proceedings of the Royal Society A: Mathematical, Physical and Engineering Sciences*, *328*(1575), 567–583. https://doi.org/10.1098/rspa.1972.0096

Pacejka, H. (2012). Tire and Vehicle Dynamics. In *Tire and Vehicle Dynamics*.

https://doi.org/10.1016/C2010-0-68548-8

Pajtas, S. R. (1990). Polyurethane Non-Pneumatic Tire Technology-Development and Testing History. *SAE Technical Paper*. https://doi.org/10.4271/900763

Rajesh Rajamani. (2006). Vehicle Dynamics and Control. In *Vehicle Dynamics and Control*. https://doi.org/10.1007/0-387-28823-6

Rao, K. V. N., & Kumar, R. K. (2007). Simulation of tire dynamic behavior using various finite element techniques. *International Journal of Computational Methods in Engineering Science and Mechanics*, *8*(5), 363–372. https://doi.org/10.1080/15502280701471566

Rhyne, T. B., & Cron, S. M. (2006). Development of a non-pneumatic wheel. *Tire Science and Technology*, *34*(3), 150–169. https://doi.org/10.2346/1.2345642

Rugsaj, R., & Suvanjumrat, C. (2018). Finite element analysis of hyperelastic material model for non-pneumatic tire. *Key Engineering Materials*, *775 KEM*, 554–559. https://doi.org/10.4028/www.scientific.net/KEM.775.554

Tönük, E., & Ünlüsoy, Y. S. (2001). Prediction of automobile tire cornering force characteristics by finite element modeling and analysis. *Computers and Structures*, *79*(13), 1219–1232. https://doi.org/10.1016/S0045-7949(01)00022-0

Veeramurthy, M., Ju, J., Thompson, L. L., & Summers, J. D. (2014). Optimisation of geometry and material properties of a non-pneumatic tyre for reducing rolling resistance. *International Journal of Vehicle Design*, *66*(2), 193–216. https://doi.org/10.1504/IJVD.2014.064567

Versace, J., & Forbes, L. (1968). *Research requirements for determining car handling characteristics*. Retrieved from http://onlinepubs.trb.org/Onlinepubs/hrr/1968/247/247-007.pdf

Wei, C., & Olatunbosun, O. A. (2017). Prediction of influence of operating conditions and tyre design parameters on tyre cornering characteristics. *International Journal of Vehicle Performance*, *3*(2), 127. https://doi.org/10.1504/ijvp.2017.10003357

Wong, J. Y. (2008). *Theory of Ground Vehicle*. John Wiley & Sons, Inc.

Yang, X. (2011). *Finite element analysis and experimental investigation of tyre characteristics for developing strain-based intelligent tyre system.*

Zhang, Z. Z., Lv, J. G., Song, B., Guo, S. Y., & Gao, F. (2013). Development of non-pneumatic tire technology. *Applied Mechanics and Materials*, *427–429*, 191–194. https://doi.org/10.4028/www.scientific.net/AMM.427-429.191

Zhao, Y., Zang, L., Chen, Y., Li, B., & Wang, J. (2015). Non-pneumatic mechanical elastic wheel natural dynamic characteristics and influencing factors. *Journal of Central South University*, *22*, 1707–1715. https://doi.org/10.1007/s11771-015-2689-1

Zhou, T., Yang, X., Gao, S., & An, R. (2017). Tyre cornering stiffness finite element analysis for tyre design parameters determination. *International Journal of Vehicle Performance*, *3*(2), 167–179. https://doi.org/10.1504/IJVP.2017.083366

Zhu, M., Zhao, Y., Lin, F., Xiao, Z., & Deng, Y. (2019). Thermo-mechanical coupled modeling for numerical analyzing the influence of thermal and frictional factors on the cornering behaviors of non-pneumatic mechanical elastic wheel. *Simulation Modelling Practice and Theory*, *91*, 13–27. https://doi.org/10.1016/j.simpat.2018.11.002

CERTIFICATE OF COMPLETENESS

It is hereby certified that the dissertation submitted by NS Mubashir Jaleel, Regn No. **00000238712**, Titled: ***Modeling and Analysis of Non-Pneumatic Tires for Military Wheeled Vehicles*** has been checked/reviewed and its contents are complete in all respects.

Supervisor's Name: **Dr. Raja Amer Azim** Signature: _____

Date: _____